

Mathematical Models and Methods in Applied Sciences
© World Scientific Publishing Company

Convergence analysis of the time-stepping numerical methods for time-fractional nonlinear subdiffusion equations

Hui Zhang

*School of Mathematics, Shandong University,
Jinan 250100, PR China
zhangh@sdu.edu.cn*

Fanhai Zeng *

*School of Mathematics, Shandong University,
Jinan 250100, PR China
fanhai_zeng@sdu.edu.cn*

Xiaoyun Jiang

*School of Mathematics, Shandong University,
Jinan 250100, PR China
wqjxyf@sdu.edu.cn*

George Em Karniadakis

*Division of Applied Mathematics and Engineering, Brown University,
Providence RI, 02912
george_karniadakis@brown.edu*

Received (Day Month Year)

Revised (Day Month Year)

Communicated by (xxxxxxxxxx)

In 1986, Dixon and McKee developed a discrete fractional Grönwall inequality [Z. Angew. Math. Mech., 66 (1986), pp. 535–544], which can be seen as a generalization of the classical discrete Grönwall inequality. However, this generalized discrete Grönwall inequality and its variant [SIAM J. Numer. Anal., 57 (2019), pp. 1524–1544] have not been widely applied in the numerical analysis of the time-stepping methods for the time-fractional evolution equations. The main purpose of this paper is to show how to apply the generalized discrete Grönwall inequality to prove the convergence of a class of time-stepping numerical methods for time-fractional nonlinear subdiffusion equations, including the popular fractional backward difference type methods of order one and two, and the fractional Crank-Nicolson type methods. We obtain the optimal L^2 error estimate in space discretization for multi-dimensional problems. The convergence of the fast time-stepping numerical methods is also proved in a simple manner. The present work unifies the convergence analysis of several existing time-stepping schemes. Numerical examples are

*Corresponding author.

2 *H. Zhang et al.*

provided to verify the effectiveness of the present method.

Keywords: Time-fractional nonlinear subdiffusion equations; discrete fractional Grönwall inequality; fast time-stepping methods; convergence.

AMS Subject Classification: 26A33, 65M06, 65M12, 65M15, 35R11

1. Introduction

The aim of this paper is to analyze the convergence of the time-stepping numerical schemes for the following time-fractional nonlinear subdiffusion equation with a reaction term $f(u)$:

$$\begin{cases} {}_0^C D_t^\alpha u = \Delta u + f(u), & \text{in } \Omega \times (0, T], T > 0, \\ u = u_0, & \text{in } \bar{\Omega}, \\ u = 0, & \text{on } \partial\Omega \times [0, T], \end{cases} \quad (1.1)$$

where Ω is a convex domain in \mathbb{R}^d with a smooth boundary, Δ is the Laplace operator defined on Ω with a homogenous boundary condition, and ${}_0^C D_t^\alpha u$ is the Caputo fractional derivative of order $0 < \alpha < 1$, which is defined by

$${}_0^C D_t^\alpha u(t) = \frac{1}{\Gamma(1-\alpha)} \int_0^t u'(s)(t-s)^{-\alpha} ds. \quad (1.2)$$

We employ the Galerkin finite element method (FEM) in space approximation. The spatial approximation can also be performed by other methods, for example, if Ω is regular, then finite difference methods or spectral methods can be applied.

The non-locality of the fractional derivative operator (1.2) causes a lot of difficulty for solving (1.1). Generally speaking, the approximation of ${}_0^C D_t^\alpha u(t)$ at $t = t_n$ can be written as

$$\sum_{k=0}^n w_{n,k} u^k, \quad 0 \leq k \leq n, \quad 0 < n \leq n_T, \quad (1.3)$$

where the coefficients $w_{n,k}$ are determined by the specific numerical method for the approximation of the fractional operator.^{3,26,31,33,39,44,50} Direct computation of (1.3) is costly, requiring $O(n_T)$ active memory and $O(n_T^2)$ operations. The computational difficulty can be resolved by developing fast memory-saving algorithms.^{4,5,10,16,17,27,32,38,48,50} The non-locality of fractional operators also makes the numerical analysis of fractional partial differential equations (PDEs) much more complicated than that of local PDEs. As is well known, the discrete Grönwall inequality (see Lemma 3.3 with $\alpha \rightarrow 1$) provides a powerful tool to analyze the stability and convergence of the numerical methods for integer-order PDEs. How to develop and use the discrete fractional Grönwall type inequalities to analyze the numerical methods for fractional PDEs has been reported much less and this is the topic of this current work.

The discrete fractional Grönwall type inequalities based on the specific time-stepping methods have been established by some researchers.^{20,28,29,45} Jin et al.²⁰

established a fractional version of the discrete Grönwall type inequality based on the convolution quadrature generated by the fractional backward difference formula of order p (FBDF- p) and the L1 formula. In Refs. 28 and 29, the authors developed the discrete fractional Grönwall type inequalities based on the interpolation method, such as the L1 method generated by linear interpolation^{31,37,39} and the Alikhanov formula generated by quadratic interpolation.³ These Grönwall type inequalities have been applied to analyze the convergence of numerical methods for a variety of nonlinear fractional PDEs.^{14,20,24,25,30}

In addition to the aforementioned discrete fractional Grönwall type inequalities, there exists a generalized discrete Grönwall inequality (see Lemma 3.3) proposed in 1986 by Dixon and McKee (see Ref. 13), which can be seen as a generalization of the classical discrete Grönwall inequality and is independent of specific time-stepping methods. The generalized discrete Grönwall inequality and its variants have been widely applied to analyze the convergence of the numerical methods for the fractional ordinary differential equations and the integral equations with weakly singular kernels.^{8,9,23,49} To the best of the authors' knowledge, this generalized discrete Grönwall inequality has not been widely applied to analyze the convergence of time-stepping numerical methods for the time-fractional PDEs except for some limited works.^{2,15,21} The goal of this work is to show how to apply the generalized discrete Grönwall inequality to prove the convergence of a class of time-stepping numerical methods for time-fractional nonlinear PDEs of the form (1.1).

The main contributions of this work are listed below:

- The generalized discrete Grönwall's inequality is applied to prove the convergence of a class of fully implicit time-stepping Galerkin FEMs for (1.1), where the time direction is approximated by the convolution quadrature with correction terms. The use of the generalized discrete Grönwall inequality in this paper is very simple and straightforward; see Section 3.
- The convergence of the fast time-stepping Galerkin FEMs for (1.1) is proved. Our proof is based on the convergence of the direct computational method, which is simpler than that of the existing fast methods; see Ref. 38.

To the best of authors' knowledge, this is the first work that unifies the convergence analysis of the popular (fast) time-stepping numerical schemes for solving (1.1), including the fractional backward difference type methods of order one and two,^{33,40} the fractional Crank–Nicolson type methods,^{19,47} and the recently developed BN- θ method,⁴⁶ see Section 4.

The convolution quadrature with correction terms has been widely applied to resolve the initial singularity of the time-fractional PDEs.^{11,20,43,46} However, the convergence analysis of time-stepping schemes with correction terms is limited; the current paper presents an approach to analyze the convergence of this kind time-stepping numerical methods. The present convolution quadrature with correction terms is different from the ones in Refs. 18 and 44, where the first several steps of the schemes are corrected.

4 *H. Zhang et al.*

The main difference of the present work from the previous ones^{20,28,29,45} is that we adopt the generalized discrete Grönwall inequality to prove the convergence of the numerical methods. Our analysis is simple and straightforward, and can be extended to analyze the numerical methods for a broader class of time-fractional evolution equations.

2. The numerical schemes

2.1. Discretization of the Caputo fractional derivative

The interval $[0, T]$ is divided into $n_T \in \mathbb{N}$ subintervals with a time step size $\tau = T/n_T$ and grid points $t_n = n\tau, 0 \leq n \leq n_T$. Denote by $u^n = u^n(\cdot) = u(\cdot, t_n)$ for notational simplicity.

Assume that the solution u of (1.1) satisfies

$$u(t) - u(0) = \sum_{k=1}^m \hat{u}_k t^{\delta_k} + \tilde{u}(t) t^{\delta_{m+1}}, \quad 0 \leq t \leq T, \quad (2.1)$$

where $0 < \delta_1 < \dots < \delta_m < \delta_{m+1}$ and $\tilde{u}(t) \in L^2([0, T]; X)$. The assumption (2.1) is used in obtaining the truncation error in time discretization, which holds for the linear equation of the form (1.1). For example, if $f = u$, then $\delta_k = k\alpha$; see Ref. 34. If $f = g(\cdot, t)$, g is sufficient smooth in time, then $\delta_k \in \{\delta_{\ell,j} | \delta_{\ell,j} = \ell + j\alpha, \ell \in \mathbb{Z}^+, j \in \mathbb{N}\}$; see Refs. 11 and 34. For the time-fractional Allen–Cahn equation, i.e., $f = u(1 - u^2)$, one has $\delta_1 = \alpha$; see Ref. 43.

The following lemma is a reformulation of Lemma 3.5 in Ref. 33, which is useful in the construction of the numerical method for the Caputo fractional operator.

Lemma 2.1 (see Ref. 33). *Let $u(t) = t^\gamma, \gamma > -1$ and $0 \leq \alpha \leq 1$. Then*

$${}_0^{RL}D_t^\alpha u(t)|_{t=t_n} = \tau^{-\alpha} \sum_{k=1}^n \omega_{n-k}^{(\alpha)} u(t_k) + O(\tau^p t_n^{\gamma-p-\alpha}) + O(\tau^{\gamma+1} t_n^{-\alpha-1}),$$

where ${}_0^{RL}D_t^\alpha$ is the Riemann–Liouville fractional derivative operator defined by

$${}_0^{RL}D_t^\alpha u(t) = \frac{1}{\Gamma(1-\alpha)} \frac{d}{dt} \int_0^t (t-s)^{-\alpha} u(s) ds,$$

the convolution weights $\omega_n^{(\alpha)}$ are the coefficients of the Taylor expansion of the generating function $\omega^{(\alpha)}(z) = \sum_{n=0}^{\infty} \omega_n^{(\alpha)} z^n$, p is the convergence order that depends on the generating function $\omega^{(\alpha)}(z)$.

The widely used generating functions $\omega^{(\alpha)}(z)$ in fractional calculus include the fractional backward difference formula of order p (FBDF- p) and the generalized

Newton-Gregory formula of order p (GNGF- p), which are given by

$$\omega^{(\alpha)}(z) = \begin{cases} \left(\sum_{k=1}^p \frac{1}{k} (1-z)^k \right)^\alpha, & \text{FBDF-}p, \\ (1-z)^\alpha \sum_{k=1}^p g_{k-1} (1-z)^{k-1}, & \text{GNGF-}p. \end{cases} \quad (2.2)$$

where $g_0 = 1, g_1 = \frac{\alpha}{2}, g_2 = \frac{\alpha^2}{8} + \frac{5\alpha}{24}, g_k (k \geq 3)$ can be found in Ref. 16. Interested readers can refer to Ref. 33 for more generating functions.

Using the relationship ${}_0^C D_t^\alpha u(t) = {}_0^{RL} D_t^\alpha (u - u(0))(t)$ (see Ref. 35) and Lemma 2.1, we can obtain

$$[{}_0^C D_t^\alpha u(t)]_{t=t_n} = D_\tau^{\alpha, m} u^n - R^n, \quad (2.3)$$

where R^n is the truncation error in time and

$$D_\tau^{\alpha, m} u^n = \frac{1}{\tau^\alpha} \sum_{j=0}^n \omega_{n-j}^{(\alpha)} (u^j - u^0) + \frac{1}{\tau^\alpha} \sum_{j=1}^m w_{n,j}^{(m)} (u^j - u^0). \quad (2.4)$$

The starting weights $w_{n,j}^{(m)}$ in (2.4) are chosen such that

$$D_\tau^{\alpha, m} u^n = [{}_0^C D_t^\alpha u(t)]_{t=t_n}, \quad u = t^{\sigma_k}, \quad 1 \leq k \leq m. \quad (2.5)$$

If u satisfies (2.1) and $\sigma_k = \delta_k, 1 \leq k \leq m+1$, then Lemma 2.1 and (2.5) yield the truncation error R^n in (2.3), which satisfies

$$R^n = O(\tau^p t_n^{\sigma_{m+1}-p-\alpha}) + O(\tau^{\sigma_{m+1}+1} t_n^{-\alpha-1}), \quad (2.6)$$

where p is the convergence order that depends the generating function $\omega^{(\alpha)}(z)$.

The quadrature weights $\omega_n^{(\alpha)}$ in (2.4) can be derived much easily. For $\omega^{(\alpha)}(z)$ defined by (2.2), the recurrence formula (5) in Ref. 12 can be used to obtain $\omega_n^{(\alpha)}$. One can also used (5.1) to calculate $\omega_n^{(\alpha)}$ for $n \geq n_0, n_0$ is a suitable positive integer.

Next, we give a criterion to select σ_k and derive the starting weights $w_{n,j}^{(m)} (1 \leq j \leq m)$ when applying the time discretization method (2.4).

1) Determine σ_k in (2.4).

From the construction of the method (2.4), the optimal choice of σ_k should be $\sigma_k = \delta_k$, where δ_k are the regularity indices of the analytical solution, see (2.1). However, we may not know δ_k for a generalized nonlinear term $f(u)$.

If $f(z)$ is sufficiently smooth, then $f(u)$ can be decomposed into as $f = f_1 + f_2$, where $f_1(u) = f(u_0) + f'(u_0)(u - u_0)$ and $f_2(u) = f(u) - f_1(u)$. Let v be the solution of the following linear system

$${}_0^C D_t^\alpha v = \Delta v + f_1(v), \quad (x, t) \in \Omega \times (0, T], T > 0 \quad (2.7)$$

subject to the initial condition $v(x, 0) = u_0(x), x \in \bar{\Omega}$ and the homogenous boundary conditions. Let w be the solution of the following nonlinear system

$${}_0^C D_t^\alpha w = \Delta w + f(v + w) - f_1(v), \quad (x, t) \in \Omega \times (0, T] \quad (2.8)$$

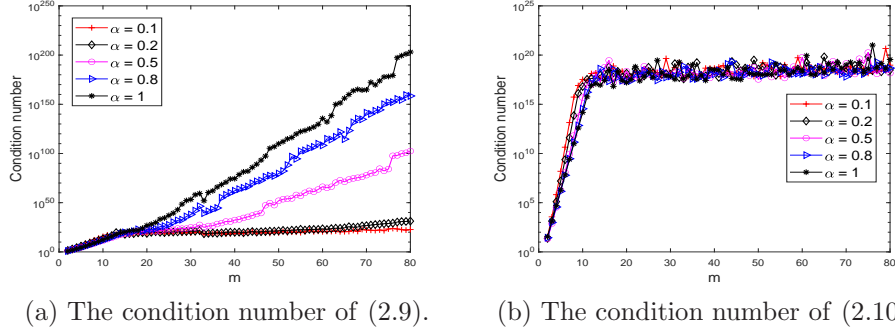
6 *H. Zhang et al.*


Fig. 1. The condition numbers of different linear systems, $\sigma_k = k\alpha$, $\tau = 0.1$. In practice, a few number of correction terms are enough to obtain accurate numerical solutions. We take $m \leq 4$ in numerical simulations in Section 6, so that the system (2.9) is relatively well-conditioned and accurate starting weights can be derived.

subject to the homogenous initial and boundary conditions. Then, the solution of (1.1) can be expressed as $u = v + w$. It is known that the analytical solution of the linear system (2.7) satisfies $v(t) - v(0) = \sum_{k=1}^m \hat{v}_k t^{\delta_k} + \tilde{v}(t)t^{\delta_{m+1}}$, where $\delta_k = k\alpha$ for $f(0) = 0$ (see Ref. 34) and $\delta_k \in \{\delta_{\ell,j} | \delta_{\ell,j} = \ell + j\alpha, \ell \in \mathbb{Z}^+, j \in \mathbb{N}\}$ for $f(0) \neq 0$ (see Ref. 11). From Ref. 43, one knows that $w(t)$ has higher regularity than $v(t)$ and $w(0) = {}_0^C D_t^\alpha w(t)|_{t=0} = 0$. Therefore, for a smooth $f(z)$, we have $\delta_1 = \alpha$, but δ_k for $k \geq 2$ need to be determined by further investigation.

Now, we know that $u(t) = v(t) + w(t)$, the regularity of $v(t)$ is known and $w(t)$ has higher regularity than $v(t)$. Hence, it is reasonable to select σ_k according to the regularity of $v(t)$, which is adopted in the current paper, and it performs well; see numerical results in Section 6.

2) Derive the starting weights $w_{n,j}^{(m)}$ ($1 \leq j \leq m$) in (2.4).

For a fixed n , the starting weights $w_{n,j}^{(m)}$ are chosen such that (2.5) holds, which yields the following linear system³³

$$\sum_{j=1}^m t_j^{\sigma_k} w_{n,j}^{(m)} = \frac{\Gamma(\sigma_k + 1)}{\Gamma(\sigma_k + 1 - \alpha)} t_n^{\sigma_k - \alpha} - \sum_{j=0}^n \omega_{n-j}^{(\alpha)} t_j^{\sigma_k}, \quad 1 \leq k \leq m. \quad (2.9)$$

Clearly, (2.9) is a Vandermonde type system, which may lead to inaccurate starting weights that may harm the accuracy of the numerical method.^{12,33,49} Diethelm et al.¹² discussed in detail how to solve the linear system (2.9) and how the starting weights and values affect the accuracy of the numerical method.

Figure 1 (a) shows the condition number of (2.9) for different fractional orders α when $\sigma_k = k\alpha$. We can see that for a smaller α , i.e., $\alpha = 0.1, 0.2$, the condition number of (2.9) increases fast as m increases up to a certain number, then it increases slowly. For a larger α , i.e., $\alpha = 0.8, 1$, the condition number increases as m increases.

One way to reduce the condition number of (2.9) is to find a suitable precondi-

tioner, which is not trivial.¹² If we can find a new basis function $\phi_k(t)$, satisfying

$$\text{span}\{t^{\sigma_1}, t^{\sigma_2}, \dots, t^{\sigma_m}\} = \text{span}\{\phi_1(t), \phi_2(t), \dots, \phi_m(t)\},$$

then the system (2.9) is equivalent to the following new system

$$\sum_{j=1}^m \phi_k(t_j) w_{n,j}^{(m)} = \int_0^{t_n} \frac{(t_n - s)^{-\alpha}}{\Gamma(1 - \alpha)} \phi_k'(s) ds - \sum_{j=0}^n \omega_{n-j}^{(\alpha)} \phi_k(t_j), \quad 1 \leq k \leq m. \quad (2.10)$$

The condition number of the new system (2.10) may become smaller if the suitable basis functions $\phi_k(t)$ are chosen.

Figure 1 (b) shows the condition number of (2.10) for $\tau = 0.1$, where we choose $\phi_k(t) = L_k^{(0)}(t^\alpha) - L_k^{(0)}(0)$, $L_k^{(\beta)}(t)$ ($\beta > -1$) is the generalized Laguerre polynomial.³⁶ We can see that for $\alpha = 0.1, 0.2, 0.5, 0.8, 1$, the condition number of (2.10) increases as m increases until it becomes about 10^{20} for $m > 10$. We have also tested other fractional orders $\alpha \in (0, 1)$ and $\tau < 0.1$, and we have obtained results similar to the ones obtained in Figure 1 (b). The condition number of (2.10) is about 10^{20} , the Multiprecision Computing Toolbox for MATLAB¹ can be used to solve (2.10), which is not costly.

In this paper, we use at most four correction terms in numerical simulations, so that the system (2.9) is relatively well-conditioned, which can be solved directly.

2.2. The fully discrete scheme

Let \mathcal{T}_h be a family of regular (conforming) triangulations of the domain $\bar{\Omega}$ and $h = \max_{K \in \mathcal{T}_h} (\text{diam}K)$. The linear finite element space X_h is defined as

$$X_h = \{v_h \in H_0^1(\Omega) : v_h|_T \text{ is a linear function } \forall T \in \mathcal{T}_h\}. \quad (2.11)$$

Define the orthogonal projectors $P_h : L^2(\Omega) \rightarrow X_h$ and $\pi_h^{1,0} : H_0^1(\Omega) \rightarrow X_h$ as

$$\begin{aligned} (P_h u, v) &= (u, v), & \forall v \in X_h, \\ (\nabla \pi_h^{1,0} u, \nabla v) &= (\nabla u, \nabla v), & \forall v \in X_h. \end{aligned}$$

where (\cdot, \cdot) is the inner product in $L^2(\Omega)$ equipped with the L^2 norm $\|\cdot\|_{L^2(\Omega)}$ and the L^∞ norm $\|\cdot\|_{L^\infty(\Omega)}$. Denote by $H^k(\Omega)$ as the Sobolev space equipped with the norm $\|\cdot\|_{H^k(\Omega)}$, $k \geq 0$. For convenience, we denote $\|\cdot\| = \|\cdot\|_{L^2(\Omega)}$.

Using (2.3), we can derive the time discretizaion for (1.1) as

$$D_\tau^{\alpha,m} u^n = \Delta u^n + f(u^n) + R^n. \quad (2.12)$$

From (2.12), the fully discrete Galerkin FEM for (1.1) may be given as: Given $u_h^0 = \pi_h^{1,0} u_0$, find $u_h^n \in X_h$ for $n \geq 1$, such that

$$(D_\tau^{\alpha,m} u_h^n, v) + (\nabla u_h^n, \nabla v) = (P_h f(u_h^n), v), \quad \forall v \in X_h. \quad (2.13)$$

8 *H. Zhang et al.*

In order to obtain the starting values $u_h^n (1 \leq n \leq m)$, we can let $n = 1, 2, \dots, m$ in (2.13), which yields a system of equations, its matrix form reads

$$A^{(m)} \begin{bmatrix} (u_h^1, v) \\ (u_h^2, v) \\ \vdots \\ (u_h^m, v) \end{bmatrix} + \tau^\alpha \begin{bmatrix} (\nabla u_h^1, \nabla v) \\ (\nabla u_h^2, \nabla v) \\ \vdots \\ (\nabla u_h^m, \nabla v) \end{bmatrix} = \tau^\alpha \begin{bmatrix} (P_h f(u_h^1), v) \\ (P_h f(u_h^2), v) \\ \vdots \\ (P_h f(u_h^m), v) \end{bmatrix}, \quad \forall v \in X_h, \quad (2.14)$$

where $A^{(m)} = \Lambda_1 V \Lambda_2 V^{-1}$, $V \in \mathbb{R}^{m \times m}$ with entries $(V)_{i,j} = i^{\sigma_j}$, $1 \leq i, j \leq m$, $\Lambda_1 = \text{diag}(1, 2^{-\alpha}, \dots, m^{-\alpha})$, $\Lambda_2 = \text{diag}(\gamma_1, \gamma_2, \dots, \gamma_m)$ with $\gamma_j = \frac{\Gamma(\sigma_j+1)}{\Gamma(\sigma_j+1-\alpha)}$, $1 \leq j \leq m$.

Generally speaking, if $A^{(m)} + (A^{(m)})^T$ is positive definite, then (2.14) permits a unique solution under some suitable conditions, which is true for $m = 1$. For $m = 2$, one has

$$A^{(2)} = \frac{1}{2^{\sigma_2} - 2^{\sigma_1}} \begin{bmatrix} \gamma_1 2^{\sigma_2} - \gamma_2 2^{\sigma_1} & \gamma_2 - \gamma_1 \\ (\gamma_1 - \gamma_2) 2^{\sigma_1 + \sigma_2 - \alpha} & \gamma_2 2^{\sigma_2 - \alpha} - \gamma_1 2^{\sigma_1 - \alpha} \end{bmatrix}.$$

It is a tedious task to find a condition to guarantee the positive definiteness of $A^{(2)} + (A^{(2)})^T$, the case for $m \geq 3$ is much more complicated. The well-posedness of (2.14) is not the main goal of this work and is not investigated.

In order to obtain a stable and convergent numerical scheme, we need to modify (2.13) to obtain a new scheme that works for all $m \geq 0$. Obviously, if $u_h^n (0 \leq n \leq m)$ are known, then (2.13) is well defined for $n \geq m + 1$.

To this end, we can modify (2.13) as: Given u_h^n for $0 \leq n \leq m$, find $u_h^n \in X_h$ for $n \geq m + 1$, such that

$$(D_\tau^{\alpha, m} u_h^n, v) + (\nabla u_h^n, \nabla v) = (P_h f(u_h^n), v), \quad \forall v \in X_h. \quad (2.15)$$

The existing numerical methods can be used to obtain $u_h^n (1 \leq n \leq m)$. For example, we can solve (2.13) with one correction term and a smaller time step size to obtain $u_h^n (1 \leq n \leq m)$, which is adopted in numerical simulations when analytical solution is unavailable. The convergence of (2.15) is given in Theorem 2.2, in which we display how the starting values affect the numerical solutions of (2.15).

In order to prove the convergence of (2.15), we define the generating functions $a^{(\alpha)}(z)$ and $b(z)$ as

$$a^{(\alpha)}(z) = (1 - z)^\alpha = \sum_{n=0}^{\infty} a_n^{(\alpha)} z^n, \quad (2.16)$$

$$b(z) = a^{(\alpha)}(z) / \omega^{(\alpha)}(z) = \sum_{n=0}^{\infty} b_n z^n. \quad (2.17)$$

Introduce the following notations:

$$\hat{b}(z) = \sum_{n=0}^{\infty} \hat{b}_n z^n, \quad \hat{b}_n = |b_n|, n \geq 0; \quad (2.18)$$

$$c(z) = (2b_0 - \hat{b}(z)) a^{(-\alpha)}(z) = \sum_{n=0}^{\infty} c_n z^n, \quad c_n = 2b_0 a_n^{(-\alpha)} - \sum_{j=0}^n \hat{b}_j a_{n-j}^{(-\alpha)}. \quad (2.19)$$

The following assumptions are used in the convergence analysis:

$$b_0 > 0, |b_n| \lesssim n^{-\alpha-1}, \sum_{n=1}^{\infty} |b_n| \leq b_0; \quad (2.20)$$

$$c_0 > 0, c_n \geq 0, n > 0, \quad (2.21)$$

where $A \lesssim B$ means there exists a positive constant C independent of τ, h , and any positive integer n , such that $A \leq CB$. In the rest of this paper, $C_k, k \in \mathbb{N}$ are generic positive constants independent of τ, h and any positive integer n .

The assumptions (2.20)–(2.21) are verified in Section 4 when the specific time discretization method is used. We have the following theorems, the proofs of which are given in Section 3.

Theorem 2.1. *Suppose that $u_0 \in H^2(\Omega) \cap H_0^1(\Omega)$, u is the solution of (1.1) satisfying (2.1), $u(t) \in H^2(\Omega) \cap H_0^1(\Omega)$, $f(u(t)) \in H^2(\Omega)$, and $|f'(z)| \lesssim 1$ for $|z| \lesssim 1$. Let $u_h^n (1 \leq n \leq n_T)$ be the solution of (2.13), $\sigma_k = \delta_k, k = 1, 2, m = 0, 1$. If the assumptions (2.20) and (2.21) hold, then*

$$\|u_h^n - u(\cdot, t_n)\| \lesssim t_n^{\alpha/2} h^2 + \tau^{\sigma_{m+1} - \alpha/2} (\ell_n^{(\sigma_{m+1})})^{1/2}, \quad (2.22)$$

where $\ell_n^{(\sigma)}$ is defined by

$$\ell_n^{(\sigma)} = \begin{cases} n^{\max\{\alpha-1, 2\sigma-2p-\alpha\}}, & \sigma \neq p + \alpha - 1/2, \\ n^{\alpha-1} \ln(n), & \sigma = p + \alpha - 1/2. \end{cases} \quad (2.23)$$

Furthermore, if $\sigma_{m+1} < p + \alpha - 1/2$, then

$$\|u_h^n - u(\cdot, t_n)\| \lesssim t_n^{\alpha/2} h^2 + \tau^{\sigma_{m+1} - \alpha/2} n^{(\alpha-1)/2}. \quad (2.24)$$

Theorem 2.2. *Suppose that $u_0 \in H^2(\Omega) \cap H_0^1(\Omega)$, u is the solution of (1.1) satisfying (2.1), $u(t) \in H^2(\Omega) \cap H_0^1(\Omega)$, $f(u(t)) \in H^2(\Omega)$, and $|f'(z)| \lesssim 1$ for $|z| \lesssim 1$. Let $u_h^n (1 \leq n \leq n_T)$ be the solution of (2.15), $\sigma_k = \delta_k, 1 \leq k \leq m + 1$. If the assumptions (2.20) and (2.21) hold, then*

$$\|u_h^n - u(\cdot, t_n)\| \leq C_1 h^2 + C_2 \tau^{\sigma_{m+1} - \alpha/2} (\ell_n^{(\sigma_{m+1})})^{1/2} + C_3 \mathcal{E}^n, \quad (2.25)$$

where $\ell_n^{(\alpha, \sigma)}$ is defined by (2.23), and \mathcal{E}^n is given by

$$\mathcal{E}^n = \tau^{\alpha/2} \left(\sum_{k=1}^m \|e^k / \tau^\alpha\| \right) (\ell_n^{(\sigma_m)})^{1/2}, \quad e^k = (u^k - u^0) - (u_h^k - u_h^0). \quad (2.26)$$

Remark 2.1. We keep \mathcal{E}^n in (2.25) in order to show how the errors of the starting values $u_h^k (1 \leq k \leq m)$ influence the accuracy of numerical solutions far from the origin. If the starting values are accurate enough, i.e., \mathcal{E}^n is sufficiently small, then we can drop \mathcal{E}^n , so that (2.25) can be simplified as

$$\|u_h^n - u(\cdot, t_n)\| \lesssim h^2 + \begin{cases} \tau^{\sigma_{m+1} - \alpha + 1/2} t_n^{(\alpha-1)/2}, & \sigma_{m+1} < p + \alpha - 1/2, \\ \tau^p \ln(n) t_n^{\sigma_{m+1} - \alpha/2 - p}, & \sigma_{m+1} = p + \alpha - 1/2, \\ \tau^p t_n^{\sigma_{m+1} - \alpha/2 - p}, & \sigma_{m+1} > p + \alpha - 1/2. \end{cases} \quad (2.27)$$

10 *H. Zhang et al.*

Remark 2.2. The error bound (2.25) also shows that \mathcal{E}^n may harm the accuracy of numerical solutions if $\ell_n^{(\sigma_m)}$ is too large. It is easy to verify that if $\sigma_m \geq p + \alpha - 1/2$, then $\ell_n^{(\sigma_m)}$ increases as σ_m increases, which makes the error induced by the starting values harm the accuracy of numerical solutions, especially when σ_m is sufficiently large; see Refs. 12 and 33.

Remark 2.3. If Ω is a rectangular domain, i.e., $\Omega = I^x \times I^y$, $I^x = (x_L, x_R)$, $I^y = (y_L, y_R)$, then the high-order bilateral element of order r can be used, and the corresponding finite element space X_h can be defined by

$$X_h = X_{h_x}^x \otimes X_{h_y}^y, \quad (2.28)$$

where

$$X_{h_\theta}^\theta = \{v : v|_{I_i^\theta} \in \mathbb{P}_r(I_i^\theta) \cap H_0^1(I^\theta)\}, \quad \theta = x, y.$$

Here $\mathbb{P}_r(I_i^\theta)$ denotes the polynomial space of order r on $I_i^\theta = [\theta_{i-1} - \theta_i]$, $\theta_i = \theta_L + (i-1)h_\theta$, $h_\theta = (\theta_R - \theta_L)/N_\theta$, $N_\theta \in \mathbb{N}$. For the two dimensional problem on the rectangular domain $\Omega = I^x \times I^y$, if the finite element space (2.11) is replaced by (2.28), then Theorem 2.1 and 2.2 hold, but the convergence rate in space changes to $O(h^{r+1})$.

3. Error estimate

In this section, we show how to apply the generalized discrete Grönwall inequality to prove Theorems 2.1 and 2.2.

3.1. Lemmas

Some useful lemmas are introduced in this subsection.

Lemma 3.1 (see Ref. 47). *Let $a^{(\beta)}(z) = (1-z)^\beta = \sum_{n=0}^{\infty} a_n^{(\beta)} z^n$, $\beta \in \mathbb{R}$, and $0 \leq \alpha \leq 1$. Then*

$$a_0^{(\alpha)} = 1, a_n^{(\alpha)} = O(n^{-\alpha-1}), a_n^{(\alpha)} \leq 0 \text{ for } n > 0, \quad 0 < -\sum_{n=1}^{\infty} a_n^{(\alpha)} \leq 1; \quad (3.1)$$

$$a_0^{(-\alpha)} = 1, a_n^{(-\alpha)} = O(n^{\alpha-1}), a_n^{(-\alpha)} \geq 0 \text{ for } n > 0; \quad (3.2)$$

$$\sum_{k=0}^n a_k^{(\alpha)} a_{n-k}^{(-\alpha)} = 0 \text{ for } n > 0. \quad (3.3)$$

The equation (3.3) can be obtained from $a^{(\alpha)}(z)a^{(-\alpha)}(z) = 1$.

Lemma 3.2. *Let $\sigma \in \mathbb{R}$ and $0 < \alpha \leq 1$. Then*

$$\sum_{j=1}^{n-1} (n-j)^{-\alpha-1} j^\sigma \lesssim n^{\max\{-\alpha-1, \sigma\}}, \quad (3.4)$$

$$\sum_{j=1}^n a_{n-j}^{(-\alpha)} j^\sigma \lesssim \begin{cases} n^{\max\{\alpha-1, \sigma+\alpha\}}, & \sigma \neq -1, \\ n^{\alpha-1} \ln(n), & \sigma = -1. \end{cases} \quad (3.5)$$

The proof of Lemma 3.2 is given in Appendix B.

Lemma 3.3 (see Ref. 2 Discrete fractional Grönwall inequality). *Assume that $\alpha > 0$, $A, B \geq 0$, and $\delta < 1$. Let z_n , $0 \leq n \leq K$, be a sequence of non-negative real numbers satisfying*

$$z_n \leq C\tau^\alpha \sum_{j=0}^{n-1} (n-j)^{\alpha-1} z_j + (A + B \log(n))t_n^{-\delta}, \quad 1 \leq n \leq K,$$

where $C > 0$ is bounded independent of τ and n . Then $z_n \lesssim (A + B \log(n))t_n^{-\delta}$.

The case of $B = \delta = 0$ in Lemma 3.3 is the original version of the discrete fractional Grönwall inequality in Ref. 13. For $B = 0$, Lemma 3.3 is equivalent to the discrete fractional Grönwall inequality (see Ref. 15 Lemma 2.1).

From Lemma 3.3, we can deduce the following corollary, which will be used in the convergence analysis instead of Lemma 3.3 for convenience.

Corollary 3.1. *Assume that $A, B \geq 0, C > 0, \delta < 1$, and $\alpha > 0$. Let z_n , $0 \leq n \leq K$, be a sequence of non-negative real numbers satisfying*

$$z_n \leq C\tau^\alpha \sum_{j=0}^n a_{n-j}^{(-\alpha)} z_j + (A + B \log(n))t_n^{-\delta}, \quad 1 \leq n \leq K.$$

If $C\tau^\alpha \leq 1/2$, i.e., $\tau \leq (2C)^{-1/\alpha}$, then $z_n \lesssim (A + B \log(n))t_n^{-\delta}$.

Proof. Using $a_0^{(-\alpha)} = 1$, $a_n^{(-\alpha)} \lesssim n^{\alpha-1}$ for $n \geq 1$, the condition $C\tau^\alpha \leq 1/2$, and Lemma 3.3 yields the desired result, which ends the proof. \square

Lemma 3.4 (see Ref. 7). *Let $0 \leq s \leq 1, s \leq r$. Then the following estimates hold*

$$\begin{aligned} \|u - \pi_h^{1,0} u\|_{H^s(\Omega)} &\lesssim h^{r-s} \|u\|_{H^r(\Omega)}, & u \in H^r(\Omega) \cap H_0^1(\Omega), \\ \|u - P_h u\|_{L^2(\Omega)} &\lesssim h^r \|u\|_{H^r(\Omega)}, & u \in H^r(\Omega). \end{aligned}$$

3.2. Proofs of Theorems 2.1 and 2.2

For the sequence $\{u^n\}_{n=1}^\infty$, $u^n \in L^2(\Omega)$, we define the following notations:

$$\mathcal{A}_\tau^{\alpha,m} u^n = \frac{1}{\tau^\alpha} \sum_{j=m+1}^n a_{n-j}^{(\alpha)} u^j, \quad (3.6)$$

$$\mathcal{B}^{\alpha,m} u^n = \sum_{j=m+1}^n b_{n-j} u^j, \quad \widehat{\mathcal{B}}^{\alpha,m} u^n = \sum_{j=m+1}^n \widehat{b}_{n-j} u^j, \quad (3.7)$$

$$W_{n,k}^{(m)} = \sum_{j=m+1}^n b_{n-j} \left(w_{j,k}^{(m)} + \omega_{j-k}^{(\alpha)} \right), \quad (3.8)$$

$$\mathcal{D}_\tau^{\alpha,m} u^n = \frac{1}{\tau^\alpha} \sum_{j=m+1}^n a_{n-j}^{(\alpha)} (u^j - u^0) + \frac{1}{\tau^\alpha} \sum_{j=1}^m W_{n,j}^{(m)} (u^j - u^0), \quad (3.9)$$

12 *H. Zhang et al.*

Lemma 3.5. *The following statements hold:*

$$\mathcal{A}_\tau^{\alpha_1, m} \mathcal{A}_\tau^{\alpha_2, m} = \mathcal{A}_\tau^{\alpha_1 + \alpha_2, m}, \quad \alpha_1, \alpha_2 \in \mathbb{R}, \quad (3.10)$$

$$\mathcal{B}^{\alpha, m} D_\tau^{\alpha, m} = \mathcal{D}_\tau^{\alpha, m}, \quad (3.11)$$

$$\mathcal{A}_\tau^{-\alpha, m} \widehat{\mathcal{B}}^{\alpha, m} \|u^n\|^2 \lesssim \mathcal{A}_\tau^{-\alpha, m} \|u^n\|^2, \quad (3.12)$$

$$(\mathcal{A}_\tau^{\alpha, m} u^n, 2u^n) \geq \mathcal{A}_\tau^{\alpha, m} \|u^n\|^2, \quad (3.13)$$

$$(\mathcal{B}^{\alpha, m} u^n, 2u^n) \geq 2b_0 \|u^n\|^2 - \widehat{\mathcal{B}}^{\alpha, m} \|u^n\|^2. \quad (3.14)$$

Proof. Eq. (3.10) can be derived from $(1-z)^{\alpha_1}(1-z)^{\alpha_2} = (1-z)^{\alpha_1+\alpha_2}$, Eq. (3.11) is derived from $b(z)\omega^{(\alpha)}(z) = (1-z)^\alpha$ and (3.8). The equality (3.12) can be deduced from (2.20), (3.2), and (3.4). The Cauchy–Schwarz inequality $2(u, v) \leq \|u\|^2 + \|v\|^2$ and (3.1) (or (2.20)) yield (3.13) (or (3.14)); see Ref. 42. The proof is completed. \square

Lemma 3.6. *Let $0 < \alpha \leq 1$, $a_n^{(-\alpha)}$ and $W_{n,k}^{(m)}$ be defined by (3.2) and (3.8), respectively. Then*

$$\sum_{j=m+1}^n a_{n-j}^{(-\alpha)} (W_{j,k}^{(m)})^2 \lesssim \ell_n^{(\sigma_m)}, \quad 1 \leq k \leq m, \quad (3.15)$$

where $\ell_n^{(\sigma_m)}$ is by (2.23).

The proof of Lemma 3.6 is given in Appendix B.

For simplicity, we assume that the nonlinear function $f(z)$ satisfies the global Lipschitz condition, i.e.,

$$|f(z_1) - f(z_2)| \lesssim |z_1 - z_2|. \quad (3.16)$$

If $f(z)$ satisfies the local Lipschitz condition, then the temporal-spatial splitting technique can be used to analyze the convergence; see Refs. 22 and 25. An alternative way to deal with the nonlinear term is to construct a function $\bar{f}(z)$, satisfying the global Lipschitz condition and $\bar{f}(z) = f(z)$ for $|z| \leq 1 + \max_{0 \leq t \leq T} \|u(t)\|_{L^\infty(\Omega)}$, where $u(t)$ is the solution of (1.1). Replacing $f(u)$ with $\bar{f}(u)$ in (2.15) (or (2.13)), one can obtain a new scheme, whose solution is also the solution of (2.15) (or (2.13)); see Refs. 6 and 43.

3.2.1. Proof of Theorem 2.1

By (3.7), (3.9), and (3.11), the scheme (2.15) can be reformulated as

$$(\mathcal{D}_\tau^{\alpha, m} u_h^n, v) + (\mathcal{B}^{\alpha, m} \nabla u_h^n, \nabla v) = (\mathcal{B}^{\alpha, m} F_h^n, v), \quad v \in X_h, \quad (3.17)$$

where $F_h^n = P_h f(u_h^n)$. Similarly, Eq. (2.12) can be written as

$$\mathcal{D}_\tau^{\alpha, m} u^n = \mathcal{B}^{\alpha, m} \Delta u^n + \mathcal{B}^{\alpha, m} F^n + \mathcal{B}^{\alpha, m} R^n, \quad F^n = f(u^n). \quad (3.18)$$

Let $\xi_h^n = \pi_h^{1,0} u^n - u_h^n$ and $\eta_h^n = \pi_h^{1,0} u^n - u^n$. From (3.17) and (3.18), we can obtain the following error equation

$$(\mathcal{D}_\tau^{\alpha, m} \xi_h^n, v) + (\mathcal{B}^{\alpha, m} \nabla \xi_h^n, \nabla v) = (\mathcal{B}^{\alpha, m} \tilde{F}_h^n, v) + (G^n + \mathcal{B}^{\alpha, m} R^n, v), \quad v \in X_h, \quad (3.19)$$

where $\tilde{F}_h^n = P_h f(\pi_h^{1,0} u^n) - P_h f(u_h^n)$ and

$$G^n = \mathcal{D}_\tau^{\alpha,m} \eta_h^n - \sum_{j=m+1}^n b_{n-j} (P_h f(\pi_h^{1,0} u^j) - f(u^j)). \quad (3.20)$$

From Lemma 3.4 and (3.16), one has

$$\|\tilde{F}_h^n\| = \|P_h(f(\pi_h^{1,0} u^n) - f(u_h^n))\| \lesssim \|f(\pi_h^{1,0} u^n) - f(u_h^n)\| \lesssim \|\xi^n\|. \quad (3.21)$$

We can similarly derive

$$\|P_h f(\pi_h^{1,0} u^j) - f(u^j)\| \leq \|P_h f(\pi_h^{1,0} u^j) - P_h f(u^j)\| + \|P_h f(u^j) - f(u^j)\| \lesssim h^2,$$

which, together with (2.20) and $\|\mathcal{D}_\tau^{\alpha,m} \eta_h^n\| \lesssim h^2$, yields

$$\|G^n\| \lesssim \|\mathcal{D}_\tau^{\alpha,m} \eta_h^n\| + \sum_{j=m+1}^n \hat{b}_{n-j} \|P_h f(\pi_h^{1,0} u^j) - f(u^j)\| \lesssim h^2. \quad (3.22)$$

From (2.6), (2.20), and (3.4), we have

$$\begin{aligned} \|\mathcal{B}^{\alpha,m} R^n\| &\lesssim \tau^{\sigma_{m+1}-\alpha} \sum_{j=m+1}^n (n+1-j)^{-\alpha-1} (j^{\sigma_{m+1}-\alpha-p} + j^{-\alpha-1}) \\ &\lesssim \tau^{\sigma_{m+1}-\alpha} (n^{\sigma_{m+1}-\alpha-p} + n^{-\alpha-1}). \end{aligned} \quad (3.23)$$

Combining (3.22), (3.23), and (3.5) yields

$$\mathcal{A}_\tau^{-\alpha,m} (\|G^n\|^2 + \|\mathcal{B}^{\alpha,m} R^n\|^2) \lesssim t_n^\alpha h^4 + \tau^{2\sigma_{m+1}-\alpha} \ell_n^{(\sigma_{m+1})}, \quad (3.24)$$

where $\ell_n^{(\sigma_{m+1})}$ is defined by (2.23).

Proof. Let $\Theta^n = \sum_{j=1}^m W_{n,j}^{(m)} \frac{\xi_h^j}{\tau^\alpha}$. By (3.6), (3.9), and $\xi_h^0 = 0$, we rewrite (3.19) as

$$(\mathcal{A}_\tau^{\alpha,m} \xi_h^n, v) + (\mathcal{B}^{\alpha,m} \nabla \xi_h^n, \nabla v) = (\mathcal{B}^{\alpha,m} \tilde{F}_h^n, v) + (G^n + \mathcal{B}^{\alpha,m} R^n - \Theta^n, v), v \in X_h. \quad (3.25)$$

The proof is finished in two steps.

Step 1) Letting $n = 1$ and $v = 2\xi_h^1$ in (3.25) yields

$$2\gamma_1 \|\xi_h^1\|^2 + 2\tau^\alpha \|\nabla \xi_h^1\|^2 = \tau^\alpha (\tilde{F}_h^1 + G^1 + R^1, 2\xi_h^1), \quad (3.26)$$

where $\gamma_1 = w_0^{(\alpha)} > 0$ for $m = 0$ and $\gamma_1 = \frac{\Gamma(\sigma_1+1)}{\Gamma(\sigma_1+1-\alpha)} > 0$ for $m = 1$. Applying the Cauchy-Schwarz inequality and $\|\tilde{F}_h^1\| \lesssim \|\xi_h^1\|$ (see (3.21)), we obtain

$$2\gamma_1 \|\xi_h^1\|^2 + 2\tau^\alpha \|\nabla \xi_h^1\|^2 \leq C_1 \tau^{2\alpha} (\|\xi_h^1\|^2 + \|G^1\|^2 + \|R^1\|^2) + \gamma_1 \|\xi_h^1\|^2. \quad (3.27)$$

If $(\gamma_1 - 2C_1 \tau^{2\alpha}) \geq 0$, i.e., $\tau \leq (2^{-1} \gamma_1 / C_1)^{1/(2\alpha)}$, then (3.27) leads to

$$\begin{aligned} \gamma_1 \|\xi_h^1\|^2 + 4\tau^\alpha \|\nabla \xi_h^1\|^2 &\leq -(\gamma_1 - 2C_1 \tau^{2\alpha}) \|\xi_h^1\|^2 + 2C_1 \tau^{2\alpha} (\|G^1\|^2 + \|R^1\|^2) \\ &\leq 2C_1 \tau^{2\alpha} (\|G^1\|^2 + \|R^1\|^2). \end{aligned} \quad (3.28)$$

Combining $R^1 = O(\tau^{\sigma_2-\alpha})$, (3.22), and (3.28) yields

$$\|\xi_h^1\|^2 \lesssim \tau^{2\alpha} (\|G^1\|^2 + \|R^1\|^2) \lesssim \tau^{2\alpha} h^4 + \tau^{2\sigma_{m+1}}. \quad (3.29)$$

14 *H. Zhang et al.*

Step 2) For $n \geq m + 1$, we can take $v = 2\xi_h^n$ in (3.25) and use (3.13)–(3.14) to obtain

$$\begin{aligned}
 & \mathcal{A}_\tau^{\alpha,m} \|\xi_h^n\|^2 + 2b_0 \|\nabla \xi_h^n\|^2 - \widehat{\mathcal{B}}^{\alpha,m} \|\nabla \xi_h^n\|^2 \\
 & \leq (\mathcal{B}^{\alpha,m} \widetilde{F}_h^n, 2\xi_h^n) + (G^n + \mathcal{B}^{\alpha,m} R^n - \Theta^n, 2\xi_h^n) \\
 & \leq \sum_{j=m+1}^n \hat{b}_{n-j} (\|\widetilde{F}_h^j\|^2 + \|\xi_h^n\|^2) + \|G^n + \mathcal{B}^{\alpha,m} R^n - \Theta^n\|^2 + \|\xi_h^n\|^2 \\
 & \leq C_2 \widehat{\mathcal{B}}^{\alpha,m} \|\xi_h^n\|^2 + (1 + 2b_0) \|\xi_h^n\|^2 + 3\rho^n,
 \end{aligned} \tag{3.30}$$

where we used $\sum_{j=1}^n \hat{b}_{n-j} \leq 2b_0$ and $\|\widetilde{F}_h^j\| \lesssim \|\xi_h^j\|$, and ρ^n is given by

$$\rho^n = \|G^n\|^2 + \|\mathcal{B}^{\alpha,m} R^n\|^2 + \|\Theta^n\|^2. \tag{3.31}$$

Applying $\mathcal{A}_\tau^{-\alpha,m}$ on both sides of (3.30), using $\mathcal{A}_\tau^{-\alpha,m} \mathcal{A}_\tau^{\alpha,m} \|\xi_h^n\|^2 = \mathcal{A}_\tau^{0,m} \|\xi_h^n\|^2 = \|\xi_h^n\|^2$ (see (3.10)) and (2.19), we obtain

$$\begin{aligned}
 & \|\xi_h^n\|^2 + \tau^\alpha \sum_{j=m+1}^n c_{n-j} \|\nabla \xi_h^j\|^2 \\
 & = \mathcal{A}_\tau^{-\alpha,m} \mathcal{A}_\tau^{\alpha,m} \|\xi_h^n\|^2 + \mathcal{A}_\tau^{-\alpha,m} (2b_0 \|\nabla \xi_h^n\|^2 - \widehat{\mathcal{B}}^{\alpha,1} \|\nabla \xi_h^n\|^2) \\
 & \leq C_2 \mathcal{A}_\tau^{-\alpha,m} \widehat{\mathcal{B}}^{\alpha,m} \|\xi_h^n\|^2 + (1 + 2b_0) \mathcal{A}_\tau^{-\alpha,m} \|\xi_h^n\|^2 + 3\mathcal{A}_\tau^{-\alpha,m} \rho^n.
 \end{aligned} \tag{3.32}$$

By $c_n \geq 0$ (see (2.21)) and $\mathcal{A}_\tau^{-\alpha,m} \widehat{\mathcal{B}}^{\alpha,m} \|\xi_h^n\|^2 \lesssim \mathcal{A}_\tau^{-\alpha,m} \|\xi_h^n\|^2$ (see (3.12)), we obtain

$$\|\xi_h^n\|^2 + c_0 \tau^\alpha \|\nabla \xi_h^n\|^2 \leq C_3 \mathcal{A}_\tau^{-\alpha,m} (\|\xi_h^n\|^2 + c_0 \tau^\alpha \|\nabla \xi_h^n\|^2) + 3\mathcal{A}_\tau^{-\alpha,m} \rho^n. \tag{3.33}$$

If $\tau \leq (2C_3)^{-1/\alpha}$, then we can apply Corollary 3.1 to obtain

$$\|\xi_h^n\|^2 \lesssim \|\xi_h^n\|^2 + c_0 \tau^\alpha \|\nabla \xi_h^n\|^2 \lesssim \mathcal{A}_\tau^{-\alpha,m} \rho^n. \tag{3.34}$$

From (3.15) and (3.24), we have

$$\begin{aligned}
 \mathcal{A}_\tau^{-\alpha,m} \rho^n & = \mathcal{A}_\tau^{-\alpha,m} (\|G^n\|^2 + \|\mathcal{B}^{\alpha,m} R^n\|^2 + \|\Theta^n\|^2) \\
 & \lesssim t_n^\alpha h^4 + \tau^{2\sigma_{m+1}-\alpha} \ell_n^{(\sigma_{m+1})} + \tau^\alpha \ell_n^{(\sigma_m)} \sum_{k=1}^m \|\xi^k / \tau^\alpha\|^2.
 \end{aligned} \tag{3.35}$$

Combing (3.34), (3.35), and (3.29), and using $\ell_n^{(\sigma_m)} \leq \ell_n^{(\sigma_{m+1})}$, we have

$$\|\xi_h^n\|^2 \lesssim t_n^\alpha h^4 + \tau^{2\sigma_{m+1}-\alpha} \ell_n^{(\sigma_{m+1})}. \tag{3.36}$$

Using (3.34), $\|u_h^n - u(\cdot, t_n)\| \leq \|\eta_h^n\| + \|\xi_h^n\|$, and $\|\eta_h^n\| \lesssim h^2$ yields (2.22), which completes the proof. \square

3.2.2. Proof of Theorem 2.2

Similar to (3.19), the error equation of (2.15) reads as

$$(\mathcal{A}_\tau^{\alpha,m} \xi_h^n, v) + (\mathcal{B}^{\alpha,m} \nabla \xi_h^j, \nabla v) = (\mathcal{B}^{\alpha,m} \tilde{F}_h^n, v) + (H^n + \mathcal{B}^{\alpha,m} R^n - \Phi^n, v), \quad (3.37)$$

where $\Phi^n = \sum_{j=1}^m W_{n,j}^{(m)}(e^j / \tau^\alpha)$, $e^j = (u^j - u^0) - (u_h^j - u_h^0)$, and

$$\|H^n\| = \|\mathcal{A}_\tau^{\alpha,m} \eta_h^n - \sum_{j=m+1}^n b_{n-j}(P_h f(\pi_h^{1,0} u^j) - f(u^j))\| \lesssim h^2. \quad (3.38)$$

The error equation (3.37) is very similar to (3.25). We can immediately obtain the convergence for the method (2.15).

Proof. From (3.34) and (3.35), we can obtain

$$\begin{aligned} \|\xi_h^n\|^2 &\lesssim \mathcal{A}_\tau^{-\alpha,m} \left(\|\mathcal{B}^{\alpha,m} R^n\|^2 + \|H^n\|^2 + \|\Phi^n\|^2 \right) \\ &\lesssim h^4 + \tau^{2\sigma_{m+1}-\alpha} \ell_n^{(\sigma_{m+1})} + \tau^\alpha \ell_n^{(\sigma_m)} \sum_{k=1}^m \|e^k / \tau^\alpha\|^2. \end{aligned} \quad (3.39)$$

Applying $\|u_h^n - u(\cdot, t_n)\| \leq \|\eta_h^n\| + \|\xi_h^n\|$ and $\|\eta_h^n\| \lesssim h^2$ completes the proof. \square

4. Applications

We present $\omega^{(\alpha)}(z)$ used in (2.4). We discuss the use of the FBDF-1 that is also known as the Grünwald–Letnikov formula, the FBDF-2, and the GNGF-2 to discretize the Caputo fractional derivative, where the generating functions $\omega^{(\alpha)}(z)$ for these methods are shown in Table 1, while the generating functions $b(z)$ and $\hat{b}(z)$ are also displayed in Table 1.

Table 1. The generating functions $\omega^{(\alpha)}(z)$, $b(z)$, and $\hat{b}(z)$.

	$\omega^{(\alpha)}(z)$	$b(z)$	$\hat{b}(z)$
FBDF-1	$(1-z)^\alpha$	1	1
FBDF-2	$(\frac{3}{2} - 2z + \frac{1}{2}z^2)^\alpha$	$(3/2 - z/2)^{-\alpha}$	$(3/2 - z/2)^{-\alpha}$
GNGF-2	$(1-z)^\alpha (1 + \frac{\alpha}{2} - \frac{\alpha}{2}z)$	$(1 + \frac{\alpha}{2} - \frac{\alpha}{2}z)^{-1}$	$(1 + \frac{\alpha}{2} - \frac{\alpha}{2}z)^{-1}$

In Examples 4.1–4.3, we verify that the assumptions (2.20) and (2.21) hold for the FBDF-1, FBDF-2, and GNGF-2.

Example 4.1 (FBDF-1). From Table 1, it is very easy to verify that the assumptions (2.20)–(2.21) hold if the FBDF-1 is used, the details are omitted.

16 *H. Zhang et al.*

Example 4.2 (FBDF-2). From Table 1, it is easy to obtain

$$\begin{aligned}\hat{b}(z) = b(z) &= (3/2 - z/2)^{-\alpha} = (3/2)^{-\alpha} \sum_{n=0}^{\infty} 3^{-n} a_n^{(-\alpha)} z^n, \\ b_n &= (3/2)^{-\alpha} 3^{-n} a_n^{(-\alpha)} \lesssim 3^{-n} \lesssim n^{-1-\alpha}, n > 0, \\ b_0 &= (2/3)^\alpha > 1 - (2/3)^\alpha = \sum_{n=1}^{\infty} \hat{b}_n.\end{aligned}$$

Hence, the assumption (2.20) holds. The proof of (2.21) is presented in Appendix A.

Example 4.3 (GNGF-2). From Table 1, it is easy to obtain

$$\begin{aligned}\hat{b}(z) = b(z) &= \left(1 + \frac{\alpha}{2} - \frac{\alpha}{2}z\right)^{-1} = \frac{2}{\alpha + 2} \sum_{n=0}^{\infty} \left(\frac{\alpha}{2 + \alpha}\right)^n z^n, \\ b_n &= \frac{2}{\alpha + 2} \left(\frac{\alpha}{2 + \alpha}\right)^n \lesssim n^{-1-\alpha}, n > 0, \\ b_0 &= \frac{2}{\alpha + 2} > 1 - \frac{2}{\alpha + 2} = \frac{\alpha}{\alpha + 2} = \sum_{n=1}^{\infty} \hat{b}_n,\end{aligned}$$

which verifies the assumption (2.20). The proof of (2.21) is presented in Appendix A.

Next, we show that the BN- θ method in Ref. 46 can be applied in the present framework. The BN- θ method recovers the FBDF-2 (or GNGF-2) if $\theta = 0$ (or $\theta = 1/2$). In the following example, we consider the BN- θ method for $0 \leq \theta \leq 1/2$.

Example 4.4 (BN- θ method). The generating functions $\omega^{(\alpha)}(z)$, $b(z)$, and $\hat{b}(z)$ are given by

$$\omega^{(\alpha)}(z) = (1 - z)^\alpha \left(\frac{3}{2} - \frac{z}{2} - \theta(1 - z)\right)^\alpha (1 + \theta\alpha(1 - z)), \quad (4.1)$$

$$b(z) = \hat{b}(z) = \frac{(1 - z)^\alpha}{\omega^{(\alpha)}(z)} = \frac{\left(\frac{3}{2} - \theta\right)^{-\alpha} \left(1 - \frac{1-2\theta}{3-2\theta}z\right)^{-\alpha}}{1 + \theta\alpha \frac{1 - \frac{\theta\alpha}{1+\theta\alpha}z}} \quad (4.2)$$

where b_n can be expressed by

$$b_n = b_0 \sum_{j=0}^n a_j^{(-\alpha)} \left(\frac{1-2\theta}{3-2\theta}\right)^j \left(\frac{\theta\alpha}{1+\theta\alpha}\right)^{n-j}, \quad b_0 = \frac{(3/2 - \theta)^{-\alpha}}{1 + \theta\alpha}. \quad (4.3)$$

Eq. (A.11) implies $b_n \lesssim 2^{-n} \lesssim n^{-1-\alpha}$ and $b_0 > \sum_{n=1}^{\infty} \hat{b}_n$ can be derived from

$$\frac{\left(1 - \frac{1-2\theta}{3-2\theta}\right)^{-\alpha}}{1 - \frac{\theta\alpha}{1+\theta\alpha}} = (1 + \theta\alpha) \left(\frac{3}{2} - \theta\right)^\alpha \leq (1 + \theta) \left(\frac{3}{2} - \theta\right) \leq \left(\frac{1+3/2}{2}\right)^2 < 2,$$

which verifies (2.20). The proof of (2.21) is presented in Appendix A.

In the rest of this section, we simply address that the two Crank-Nicolson (CN) type methods in Ref. 47 can be analyzed in the present frame work. We do not show how to obtain the CN type methods, readers can refer to Ref. 47 for details.

The CN Galerkin FEM for solving (1.1) reads as: Given $u_h^0 = \pi_h^{1,0} u_0$, find $u_h^n \in X_h$ for $n \geq 1$, such that

$$\begin{aligned} & \frac{1}{\tau^\alpha} \sum_{j=1}^n a_{n-j}^{(\alpha)} (u_h^j - u_h^0, v) + \sum_{j=1}^n b_{n-j} (\nabla u_h^j, \nabla v) \\ &= \sum_{j=1}^n b_{n-j} \left(P_h f(u_h^j), v \right) + B_n (P_h f(u_h^0), v) - B_n (\nabla u_h^0, \nabla v), \quad \forall v \in X_h, \end{aligned} \quad (4.4)$$

where B_n and b_n are given by

$$B_n = \frac{1}{\Gamma(1+\alpha)} \sum_{j=1}^n a_{n-j}^{(\alpha)} j^\alpha - \sum_{j=0}^{n-1} b_j = O(n^{-1}), \quad (4.5)$$

$$b(z) = 1 - \frac{\alpha}{2} + \frac{\alpha}{2} z \quad \text{or} \quad b(z) = 2^{-\alpha} (1+z)^\alpha. \quad (4.6)$$

If $\alpha \rightarrow 1$, (4.4) recovers the classical CN method. Obviously, the scheme (4.4) is similar to (3.17), we can follow the convergence proof of (3.17) to prove the stability and convergence of (4.4) if the assumptions (2.20) and (2.21) hold.

Next, we verify the assumptions (2.20) and (2.21), but we need to replace $b(z)$ defined by (2.17) with (4.6).

Example 4.5. For $b(z) = 1 - \frac{\alpha}{2} + \frac{\alpha}{2} z$, we have $\hat{b}(z) = b(z)$. The assumption (2.20) follows from $b_0 = 1 - \frac{\alpha}{2} \geq \frac{\alpha}{2} = \sum_{n=1}^{\infty} \hat{b}_n$. For $n = 0$, we have $c_0 = b_0 = 1 - \alpha/2 > 0$. Using $a_{n-1}^{(-\alpha)}/a_n^{(-\alpha)} = n/(n-1+\alpha) \leq \alpha^{-1}$ for $n \geq 1$ yields

$$c_n/a_n^{(-\alpha)} = 2b_0 - (b_0 + b_1 a_{n-1}^{(-\alpha)}/a_n^{(-\alpha)}) \geq (1-\alpha)/2 \geq 0,$$

which verifies (2.21).

Example 4.6. For $b(z) = 2^{-\alpha} (1+z)^\alpha$, we have $\hat{b}(z) = 2^{-\alpha} (2 - (1-z)^\alpha)$. It is straightforward to obtain

$$b_n = 2^{-\alpha} (-1)^n a_n^{(\alpha)}, \quad b_0 = 2^{-\alpha} \geq 2^{-\alpha} = \sum_{n=1}^{\infty} \hat{b}_n,$$

which verifies the assumption (2.20). For c_n , we have $c_0 = b_0 = 2^{-\alpha} > 0$ and $c_n = 0$ for $n > 0$, which verifies (2.21).

5. Fast time-stepping methods

We call (2.15) the direct method, which requires $O(n_T)$ memory and $O(n_T^2)$ computational cost in time. In this section, we first present the fast version of (2.15), which significantly reduces the memory requirement and computational cost. Then,

we propose a simple approach to prove that the fast method is convergent as the direct method.

The basic idea for fast calculating the discrete convolution $\sum_{j=0}^n \omega_{n-j}^{(\alpha)} u^j$ is to represent the convolution weight $\omega_n^{(\alpha)}$ as an integral (see Refs. 5, 16, 32, 38 and 48). We do not show how to derive the integral representation of $\omega_n^{(\alpha)}$, this is not the main goal of this work, readers can refer Refs. 16 and 32 for details. We adopt the fast method in Ref. 16 for illustration, but the fast methods in Refs. 5, 32, 38 and 48 can be applied in the present framework.

Due to $\sigma = 0$ in (4.11) of Ref. 16, the convolution weight $\omega_n^{(\alpha)}$ is expressed into

$$\omega_n^{(\alpha)} = \tau^{1+\alpha} \int_{-\infty}^{\infty} (1 + \tau e^x)^{-1-n} \phi(x) dx, \quad \phi(x) = -\frac{\sin(\alpha\pi) e^{(1+\alpha)x}}{\pi b(-e^x)}, \quad (5.1)$$

where $b(z)$ is defined by (2.17). The above integral can be approximated by the truncated trapezoidal rule given by (see Ref. 16 (4.15))

$$\omega_n^{(\alpha)} = \tilde{\omega}_n^{(\alpha)} + O(n^{-\alpha-1}\epsilon), \quad \tilde{\omega}_n^{(\alpha)} = \tau^{1+\alpha} \sum_{\ell=1}^Q \varpi_{\ell} (1 + \tau e^{\lambda_{\ell}})^{-1-n}, \quad n \geq n_0, \quad (5.2)$$

where n_0 is a suitable positive integer satisfying $n_0 > m + 1$, the quadrature point $\lambda_{\ell} = x_{\min} + (\ell-1)\Delta x$, the quadrature weight $\varpi_{\ell} = \Delta x \phi(x_{\ell})$, $\Delta x = (x_{\max} - x_{\min})/Q$, Q is the number of quadrature points satisfying $Q \ll n_T$. For a given precision ϵ , x_{\max} and x_{\min} are given by¹⁶

$$x_{\min} = \frac{\log(\epsilon)}{1+\alpha} - \log(n_T \tau), \quad x_{\max} = \log\left(\frac{-2\log(\epsilon) + 2(1+\alpha)\log(n_0 \tau)}{n_0 \tau}\right).$$

With (5.2), we define the fast convolution quadrature operator ${}_F D_{\tau}^{\alpha, m}$ as

$${}_F D_{\tau}^{\alpha, m} u^n = \frac{1}{\tau^{\alpha}} \sum_{j=n-n_0+1}^n \omega_{n-j}^{(\alpha)} (u^j - u^0) + \frac{1}{\tau^{\alpha}} \sum_{j=1}^{n-n_0} \tilde{\omega}_{n-j}^{(\alpha)} (u^j - u^0) + \frac{1}{\tau^{\alpha}} \sum_{j=1}^m w_{n,j}^{(m)} (u^j - u^0). \quad (5.3)$$

Using (5.2), we find that $\tau^{-\alpha} \sum_{j=1}^{n-n_0} \tilde{\omega}_{n-j}^{(\alpha)} (u^j - u^0)$ in (5.3) can be calculated by

$$\frac{1}{\tau^{\alpha}} \sum_{j=1}^{n-n_0} \tilde{\omega}_{n-j}^{(\alpha)} (u^j - u^0) = \sum_{\ell=1}^Q \varpi_{\ell} y_{\ell}^{n-n_0}, \quad (5.4)$$

where y_{ℓ}^n satisfies the following recurrence relation

$$y_{\ell}^n = \frac{1}{1 + \tau e^{\lambda_{\ell}}} [y_{\ell}^{n-1} + \tau(u^{n-1} - u^0)], \quad y_{\ell}^0 = 0. \quad (5.5)$$

Clearly, the discrete convolution $\frac{1}{\tau^{\alpha}} \sum_{j=1}^{n-n_0} \tilde{\omega}_{n-j}^{(\alpha)} (u^j - u^0)$ in (5.3) is reformulated as (5.4), which requires $O(Q)$ storage and $O(Qn_T)$ computational cost.

We replace $D_{\tau}^{\alpha, m}$ in (2.15) with ${}_F D_{\tau}^{\alpha, m}$ to obtain the fast time-stepping Galerkin FEM for (1.1) as: Find ${}_F u_h^n \in X_h$ for $n \geq n_0 > m + 1$, such that

$$\begin{cases} ({}_F D_{\tau}^{\alpha, m} {}_F u_h^n, v) + (\nabla {}_F u_h^n, \nabla v) = (P_h f({}_F u_h^n), v), & \forall v \in X_h, \\ {}_F u_h^j = u_h^j, & 0 \leq j \leq n_0 - 1, \end{cases} \quad (5.6)$$

where u_h^j is the solution of the direct method (2.15) and ${}_F D_\tau^{\alpha,m}$ is defined by (5.4).

According to Refs. 16 and 41, $\tilde{\omega}_n^{(\alpha)}$ can be expressed by

$$\tilde{\omega}_n^{(\alpha)} = (1 + \varepsilon_n)\omega_n^{(\alpha)}, \quad (5.7)$$

where ε_n is the error that can be made arbitrarily small and $\varepsilon_n = 0$ for $0 \leq n < n_0$.

We have the following theorem, the proof of which is given in Appendix C.

Theorem 5.1. *Let u_h^n and ${}_F u_h^n$ be the solutions of (2.15) and (5.6), respectively. If the conditions in Theorem 2.2 hold, $m \leq n_0$, and $|\varepsilon_n| \lesssim \tau^\alpha \varepsilon$, then*

$$\|{}_F u_h^n - u_h^n\| \lesssim \varepsilon. \quad (5.8)$$

6. Numerical results

In this section, we perform numerical experiments to verify the efficiency of the scheme (2.15). We focus on the following two aspects:

- Verify the accuracy and convergence of the scheme (2.15) when the regularity of the analytical solution is known, i.e., δ_k is known. In such a case, the optimal choice of σ_k should be $\sigma_k = \delta_k$; see Tables 2–3.
- If the regularity of the analytical solution is unknown, the method (2.15) still works well by choosing suitable σ_k . For example, select $\sigma_k = k\alpha$ or $\sigma_k \in \{\sigma_{\ell,j} | \sigma_{\ell,j} = \ell + j\alpha, \ell \in Z^+, j \in Z^+\}$, accurate numerical solutions can still be obtained, the related numerical results are shown in Tables 4–9.

At most four correction terms are used to achieve accurate numerical solutions, which verifies that the present time-stepping (2.15) is efficient. This also demonstrates that Lubich’s convolution quadrature with correction terms³³ is practically valuable.

Example 6.1. Consider the time-fractional subdiffusion equation

$$\begin{cases} {}_0^C D_t^\alpha u = \frac{1}{2\pi^2} \Delta u + f(u), & (x, t) \in \Omega \times (0, T], T > 0, \\ u(x, y, 0) = \sin(\pi x) \sin(\pi y), & (x, y) \in \bar{\Omega}, \\ u(x, y, t) = 0, & (x, y, t) \in \partial\Omega \times [0, T], \end{cases} \quad (6.1)$$

where $\Delta = \partial_x^2 + \partial_y^2$, $(x, y) \in \Omega := (0, 1)^2$, and $0 < \alpha \leq 1$.

- Case I: $f = 0$, the exact solution of (6.1) is $u = E_\alpha(-t^\alpha) \sin(\pi x) \sin(\pi y)$, where $E_\alpha(z)$ is the Mittag–Leffler function defined by $E_\alpha(z) = \sum_{k=0}^{\infty} \frac{z^k}{\Gamma(k\alpha+1)}$.
- Case II: $f = u(1 - u^2)$, the exact solution of (6.1) is unknown.

We choose the FBDF-2 in time discretization, i.e., $\omega^{(\alpha)}(z) = (3/2 - 2z + z^2/2)^\alpha$ with $p = 2$, and the bicubic element in space approximation, i.e., $r = 3$ in (2.28). The space step size is taken as $h = 1/128$. The error at $t = t_n$ is denoted by

$$e^n = u(t_n) - u_h^n.$$

20 *H. Zhang et al.*

If the analytical solution is unavailable, then the reference solution is obtained from the corresponding fast method (5.6) with one correction term and a smaller time stepsize $\tau = 2^{-17}$. The starting values used in (2.15) for $m \geq 2$ is obtained by solving (2.13) with a step size $10^{-1}\tau/\lceil\tau^{-1}\rceil$ and $m = 1$. We only show the accuracy in time.

For Case I, the exact solution is known, we have $\delta_k = k\alpha$, so σ_k used in (2.15) is chosen as $\sigma_k = k\alpha$. By (2.27), the temporal error at $t = t_n \gg 0$ is $O(\tau^2)$ for $m\alpha > 1.5$, $O(\tau^2 \log(n))$ for $m\alpha = 1.5$, and $O(\tau^{m\alpha+0.5})$ for $m\alpha < 1.5$.

Table 2 shows the L^2 errors for $\alpha = 0.2, 0.5$ and 0.8 at $t = 1$. For $\alpha = 0.2$, the regularity of the analytical solution is low, but the accuracy of the numerical solutions increases significantly as the number of correction terms increases up to four, and the observed convergence rate is better than the theoretical result $O(\tau^{m\alpha+0.5})$. Second-order accuracy can be obtained if we increase m and use the quadruple-precision in computations, which seems unnecessary for numerical practices, since four correction terms with double precision can achieve sufficiently accurate numerical results. As α increases, the regularity of the analytical solution improves, three/two correction terms are enough to achieve second-order accuracy for $\alpha = 0.5/0.8$, which agrees with the theoretical analysis. However, better convergence rate is observed than the theoretical convergence rate $O(\tau^{m\alpha+0.5})$ for $m\alpha < 1.5$. Table 3 shows the maximum L^2 errors for $\alpha = 0.2, 0.5$ and 0.8 . We observe that the accuracy of numerical solutions increases significantly as the number of the correction terms increases, especially for a smaller fractional order α , though the theoretical convergence of the maximum L^2 error is $O(\tau^{(m+0.5)\alpha})$. Both Tables 2 and 3 demonstrate that a few number of corrections are enough to achieve accurate numerical solutions, which will be further verified in Case II for solving nonlinear problems.

Table 2. The L^2 error at $t = 1$ for Case I, $\sigma_k = k\alpha, \tau = 2^{-J}$.

α	J	$m = 0$	rate	$m = 1$	rate	$m = 2$	rate	$m = 3$	rate	$m = 4$	rate
0.2	5	3.98e-4		2.63e-5		4.33e-6		6.93e-7		7.08e-8	
	6	1.98e-4	1.00	1.19e-5	1.14	1.75e-6	1.31	2.42e-7	1.52	2.52e-8	1.49
	7	9.91e-5	1.00	5.37e-6	1.15	7.00e-7	1.32	8.51e-8	1.51	9.45e-9	1.42
	8	4.95e-5	1.00	2.39e-6	1.17	2.78e-7	1.33	3.01e-8	1.50	3.54e-9	1.41
	9	2.47e-5	1.00	1.06e-6	1.17	1.10e-7	1.34	1.07e-8	1.49	1.30e-9	1.45
0.5	5	1.08e-3		1.16e-5		2.50e-6		8.09e-6		7.39e-6	
	6	5.36e-4	1.01	4.00e-6	1.54	8.39e-7	1.58	2.31e-6	1.81	2.61e-6	1.50
	7	2.67e-4	1.00	1.43e-6	1.49	2.51e-7	1.74	6.34e-7	1.87	8.21e-7	1.67
	8	1.34e-4	1.00	5.13e-7	1.47	7.07e-8	1.83	1.69e-7	1.91	2.40e-7	1.77
	9	6.67e-5	1.00	1.85e-7	1.47	1.92e-8	1.88	4.41e-8	1.94	6.70e-8	1.84
0.8	5	2.03e-3		6.96e-5		2.72e-5		3.43e-5		1.90e-5	
	6	1.01e-3	1.01	1.98e-5	1.82	7.05e-6	1.95	9.50e-6	1.85	5.83e-6	1.70
	7	5.02e-4	1.01	5.59e-6	1.82	1.80e-6	1.97	2.51e-6	1.92	1.63e-6	1.84
	8	2.50e-4	1.00	1.58e-6	1.82	4.58e-7	1.98	6.48e-7	1.95	4.34e-7	1.91
	9	1.25e-4	1.00	4.46e-7	1.82	1.16e-7	1.99	1.65e-7	1.97	1.12e-7	1.95

Next, we numerically display how σ_k influence the accuracy of numerical so-

Table 3. The maximum L^2 error $\max_{1 \leq n \leq T/\tau} \|e^n\|$ for Case I, $\sigma_k = k\alpha, T = 1, \tau = 2^{-J}$.

α	J	$m = 0$	rate	$m = 1$	rate	$m = 2$	rate	$m = 3$	rate	$m = 4$	rate
0.2	5	2.07e-2		2.75e-4		2.35e-5		4.97e-6		5.14e-7	
	6	1.95e-2	0.09	2.36e-4	0.22	1.83e-5	0.36	3.56e-6	0.48	3.32e-7	0.63
	7	1.82e-2	0.10	2.00e-4	0.24	1.40e-5	0.38	2.49e-6	0.51	2.10e-7	0.66
	8	1.69e-2	0.11	1.68e-4	0.25	1.06e-5	0.41	1.71e-6	0.54	1.29e-7	0.70
	9	1.56e-2	0.12	1.40e-4	0.27	7.88e-6	0.43	1.16e-6	0.57	7.81e-8	0.73
0.5	5	2.29e-2		1.46e-4		2.30e-5		1.21e-5		7.39e-6	
	6	1.71e-2	0.42	7.64e-5	0.94	1.08e-5	1.10	4.28e-6	1.50	2.61e-6	1.50
	7	1.26e-2	0.44	3.89e-5	0.98	4.66e-6	1.21	1.41e-6	1.60	8.21e-7	1.67
	8	9.12e-3	0.46	1.95e-5	1.00	1.90e-6	1.29	4.43e-7	1.67	2.40e-7	1.77
	9	6.58e-3	0.47	9.70e-6	1.01	7.45e-7	1.35	1.33e-7	1.73	6.70e-8	1.84
0.8	5	1.08e-2		1.16e-4		3.76e-5		3.43e-5		1.90e-5	
	6	6.43e-3	0.75	3.76e-5	1.62	1.04e-5	1.85	9.50e-6	1.85	5.83e-6	1.70
	7	3.77e-3	0.77	1.21e-5	1.63	2.79e-6	1.91	2.51e-6	1.92	1.63e-6	1.84
	8	2.19e-3	0.78	3.93e-6	1.63	7.26e-7	1.94	6.48e-7	1.95	4.34e-7	1.91
	9	1.26e-3	0.79	1.27e-6	1.62	1.86e-7	1.96	1.65e-7	1.97	1.12e-7	1.95

lutions when $\sigma_k \notin \{\delta_1, \delta_2, \dots, \delta_m, \dots\}$. In such a case, the discretization error in time is $O(\tau^{0.5} t_n^{(\alpha-1)/2})$ by Theorem 2.2. We consider Case I and take $\alpha = 0.2$ and $\sigma_k = 10^{-1}(2k - 1)$ in numerical simulations. Table 4 displays the L^2 errors at $t = 1$, where we observe about first-order accuracy for all $0 \leq m \leq 4$. What is interesting is that the error still decreases significantly as m increases, though the convergence rate is almost not improved. Similar results in Table 5 are observed, where the maximum L^2 errors are displayed. This phenomenon was studied in Ref. 49, which could be simply explained from the fact that the time discretization (2.12) (see also (2.3)) is exact for $u = t^{\sigma_k}$. Since $\sigma_k \notin \{\delta_1, \delta_2, \delta_3, \dots\}$, the leading term of the time discretization error, which we denote as $R_0^n(\delta_1) = R_0^n(\sigma_1, \sigma_2, \dots, \sigma_m, \delta_1)$, depends on t^{δ_1} (or δ_1). From (2.5), one knows that $R_0^n(\delta) = 0$ for all $\delta \in \{\sigma_1, \sigma_2, \dots, \sigma_m\}$ and $R_0^n(\delta)$ is an analytical function with respect to δ . Hence, it is reasonable to believe that $|R_0^n(\delta)|$ contains the factor $S_m(\delta) = \prod_{k=1}^m |\delta - \sigma_k|$ and $S_m(\delta)$ may be small. For Case I, $\alpha = 0.2$ and $\sigma_k = 10^{-1}(2k - 1)$, one has $\delta_1 = 0.2$, $S_1(\delta_1) = 10^{-1}$, $S_2(\delta_1) = 10^{-2}$, $S_3(\delta_1) = 3 \times 10^{-3}$, and $S_4(\delta_1) = 1.5 \times 10^{-3}$. From Tables 4–5, we indeed observe that the accuracy increases as $S_m(\delta_1)$ decreases. Even if the regularity of the analytical solution is unknown, adding suitable correction terms may help improve the accuracy of the numerical solutions; see also related results in Tables 6–7 and Tables 3 and 10, and Fig. 2.2. of Ref. 49.

Table 4. The L^2 error $\|e^n\|$ at $t = 1$ for Case I, $\alpha = 0.2, \sigma_k = (2k - 1)/10$.

$1/\tau$	$m = 0$	rate	$m = 1$	rate	$m = 2$	rate	$m = 3$	rate	$m = 4$	rate
32	3.98e-4		1.97e-5		8.75e-6		2.81e-6		9.63e-7	
64	1.98e-4	1.00	1.12e-5	0.82	4.37e-6	1.00	1.32e-6	1.09	4.68e-7	1.04
128	9.91e-5	1.00	6.19e-6	0.85	2.17e-6	1.01	6.26e-7	1.08	2.27e-7	1.05
256	4.95e-5	1.00	3.37e-6	0.88	1.07e-6	1.02	2.97e-7	1.08	1.09e-7	1.06
512	2.47e-5	1.00	1.80e-6	0.90	5.23e-7	1.03	1.41e-7	1.07	5.17e-8	1.07

Table 5. The maximum L^2 error $\max_{1 \leq n \leq T/\tau} \|e^n\|$ for Case I, $\alpha = 0.2, \sigma_k = (2k - 1)/10$.

$1/\tau$	$m = 0$	rate	$m = 1$	rate	$m = 2$	rate	$m = 3$	rate	$m = 4$	rate
32	2.07e-2		1.88e-4		5.82e-5		1.89e-5		4.60e-6	
64	1.95e-2	0.09	2.04e-4	-0.12	5.57e-5	0.06	1.74e-5	0.12	4.10e-6	0.17
128	1.82e-2	0.10	2.15e-4	-0.07	5.25e-5	0.09	1.57e-5	0.14	3.61e-6	0.18
256	1.69e-2	0.11	2.20e-4	-0.04	4.88e-5	0.10	1.41e-5	0.16	3.17e-6	0.19
512	1.56e-2	0.12	2.21e-4	-0.01	4.51e-5	0.12	1.25e-5	0.17	2.77e-6	0.20

For Case II, we know $\delta_1 = \alpha$, but we do not exactly know δ_k for $k \geq 2$. Based on the criteria on selecting σ_k (see lines below (2.8)), we take $\sigma_k = k\alpha$ in numerical simulations.

Take $\alpha = 0.2$, the L^2 errors at $t = 1$ and the maximum L^2 errors are displayed in Tables 6 and 7, respectively. We can see that the accuracy is improved significantly as m increases, though the regularity of the solution is unknown.

Table 6. The L^2 error $\|e^n\|$ at $t = 1$ for Case II, $\alpha = 0.2, \sigma_k = k\alpha, k \leq 4$.

$1/\tau$	$m = 0$	rate	$m = 1$	rate	$m = 2$	rate	$m = 3$	rate	$m = 4$	rate
32	2.01e-4		1.48e-5		3.20e-6		7.56e-7		1.69e-7	
64	1.00e-4	1.00	6.93e-6	1.10	1.39e-6	1.21	3.02e-7	1.33	7.35e-8	1.20
128	5.00e-5	1.00	3.20e-6	1.11	5.94e-7	1.22	1.21e-7	1.31	3.23e-8	1.19
256	2.50e-5	1.00	1.47e-6	1.12	2.53e-7	1.23	4.90e-8	1.31	1.39e-8	1.22
512	1.25e-5	1.00	6.70e-7	1.13	1.07e-7	1.24	1.96e-8	1.32	5.66e-9	1.30

Table 7. The maximum L^2 error $\max_{1 \leq n \leq T/\tau} \|e^n\|$ for Case II, $\alpha = 0.2, \sigma_k = k\alpha, k \leq 4, T = 1$.

$1/\tau$	$m = 0$	rate	$m = 1$	rate	$m = 2$	rate	$m = 3$	rate	$m = 4$	rate
32	9.58e-3		1.43e-4		1.77e-5		5.52e-6		1.09e-6	
64	9.01e-3	0.09	1.26e-4	0.18	1.50e-5	0.24	4.61e-6	0.26	8.94e-7	0.28
128	8.44e-3	0.10	1.11e-4	0.19	1.26e-5	0.24	3.85e-6	0.26	7.33e-7	0.29
256	7.86e-3	0.10	9.69e-5	0.20	1.06e-5	0.25	3.21e-6	0.26	5.90e-7	0.31
512	7.29e-3	0.11	8.42e-5	0.20	8.93e-6	0.25	2.64e-6	0.28	4.53e-7	0.38

Table 8 displays the L^2 errors at $t = 1$ for $\alpha = 0.8$, the accuracy increases as m increases up to two, about second-order accuracy is observed when $m = 2$. For $m \geq 3$, the accuracy decreases as m increases, which could be explained from (2.25), where the error \mathcal{E}^n induced by the starting values dominates the overall accuracy and increases as m increases when $m \geq 2$; see Remark 2.2. Direct computation shows $\ell_n^{(\sigma_1)} = \ell_n^{(\sigma_2)} = n^{-0.2}$, $\ell_n^{(\sigma_3)} = 1$, and $\ell_n^{(\sigma_4)} = n^{1.6}$. The negative effect caused by $\ell_n^{(\sigma_m)}$ for $m = 3, 4$ is observed in Table 8.

We also take $\alpha = 0.8$, but select $\sigma_k \in \{\sigma_{\ell,j} | \sigma_{\ell,j} = \ell + j\alpha, \ell \in \mathbb{Z}^+, j \in \mathbb{Z}^+\}$ in numerical simulations, i.e., $\sigma_1 = 0.8, \sigma_2 = 1, \sigma_3 = 1.6$ and $\sigma_4 = 1.8$. From Table 9, we can see that second-order accuracy is observed for $m \geq 3$. Although we cannot

claim that the solution contains t , $t^{1.6}$, and $t^{1.8}$, what we observe is that the selected σ_k can help to improve the accuracy of numerical solutions.

We find that the analytical solution possibly contains the term $t^{2\alpha}$ (see $m = 2$ in Table 8 and $m = 3$ in Table 9), since the accuracy is improved significantly when $t^{2\alpha}$ is exactly calculated in the numerical method.

Table 8. The L^2 error $\|e^n\|$ at $t = 1$ for Case II, $\alpha = 0.8, \sigma_k = k\alpha$.

$1/\tau$	$m = 0$	rate	$m = 1$	rate	$m = 2$	rate	$m = 3$	rate	$m = 4$	rate
32	1.02e-3		5.60e-5		1.75e-5		1.71e-4		7.36e-4	
64	5.07e-4	1.01	1.64e-5	1.77	4.74e-6	1.88	5.81e-5	1.56	3.27e-4	1.17
128	2.52e-4	1.01	4.74e-6	1.79	1.26e-6	1.91	1.76e-5	1.72	1.18e-4	1.47
256	1.26e-4	1.00	1.36e-6	1.80	3.32e-7	1.92	4.94e-6	1.83	3.69e-5	1.67
512	6.29e-5	1.00	3.90e-7	1.80	8.90e-8	1.90	1.32e-6	1.90	1.06e-5	1.80

Table 9. The L^2 error $\|e^n\|$ at $t = 1$ for Case II, $\alpha = 0.8, \sigma_1 = 0.8, \sigma_2 = 1, \sigma_3 = 1.6, \sigma_4 = 1.8$.

$1/\tau$	$m = 0$	rate	$m = 1$	rate	$m = 2$	rate	$m = 3$	rate	$m = 4$	rate
32	1.02e-3		5.60e-5		1.59e-5		1.50e-5		2.29e-5	
64	5.07e-4	1.01	1.64e-5	1.77	5.45e-6	1.54	4.48e-6	1.74	6.54e-6	1.81
128	2.52e-4	1.01	4.73e-6	1.79	1.74e-6	1.65	1.24e-6	1.85	1.46e-6	2.16
256	1.26e-4	1.00	1.35e-6	1.81	5.28e-7	1.72	3.27e-7	1.92	2.82e-7	2.37
512	6.29e-5	1.00	3.83e-7	1.82	1.54e-7	1.78	8.36e-8	1.97	5.53e-8	2.35

Finally, we display the numerical solutions for Case II at $t = 1, 5, 10, 20$, see Figure 2. For the selected computational domain and initial data, we observe that the solution decays as time t evolves and it decays faster as the fractional order α increases.

7. Conclusion and discussion

In this paper, we show how to apply the generalized discrete Grönwall’s inequality to prove the convergence of a class of fully implicit time-stepping Galerkin FEM for the one-dimensional nonlinear subdiffusion equations. The correction terms are used to deal with the initial singularity of the solution. The convergence analysis for this kind of time-stepping schemes is limited, hence this work provides a simple approach to the convergence of the time-stepping schemes with correction terms. We also show a simple way to prove the convergence of the fast time-stepping Galerkin FEM based on the convergence of the direct time-stepping schemes. It is hopeful that the methodology used in the convergence analysis of the present fast method can be extended to simplify the convergence analysis in Refs. 17 and 50.

If the nonlinear term $f(u^n)$ is approximated by the first-order extrapolation $f(u^{n-1})$ or second-order extrapolation $2f(u^{n-1}) - f(u^{n-2})$, then we obtain the semi-implicit time-stepping FEMs, the convergence of which can be obtained directly.

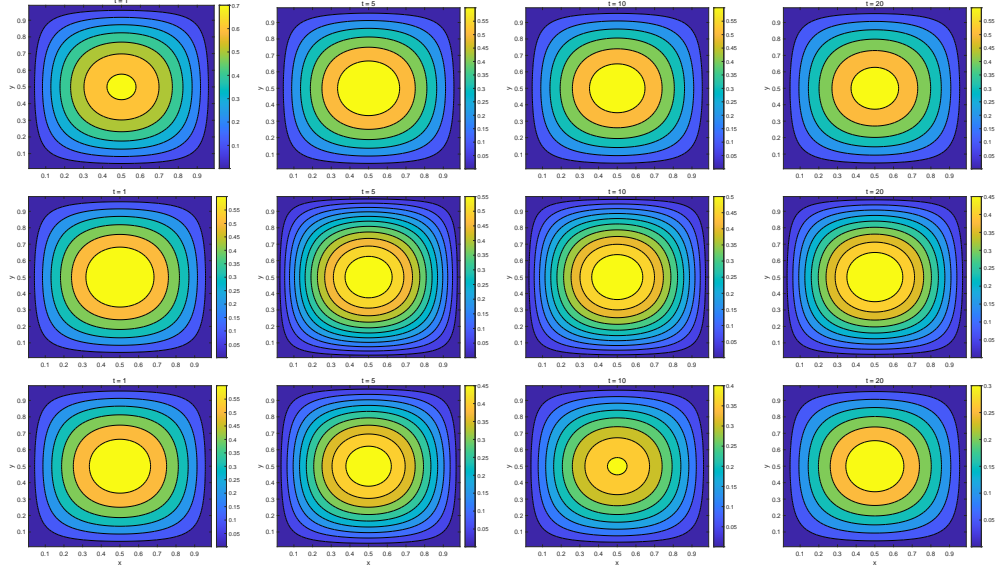
24 *H. Zhang et al.*

Fig. 2. Numerical solutions for Case II, $\tau = 0.01, h = 1/32, m = 1, \alpha = 0.2, 0.5, 0.8$ (from top to bottom), and $t = 1, 5, 10, 20$ (from left to right).

The convergence analysis in this paper is very simple, so hopefully it can be extended to analyze the convergence of numerical methods for the complicated time-fractional evolution equations.

The observed convergence rate is better than that from the theoretical analysis when $\sigma_{m+1} < p + \alpha - 1/2$. Other techniques are needed in convergence analysis, which will be studied in our future work.

Appendix A. Proof of $c_n \geq 0$ for the BN- θ method

The BN- θ method reduces to the FBDF-2 method for $\theta = 0$ and to the GNGF-2 for $\theta = 1/2$. In this section, we prove $c_n \geq 0$ for the BN- θ method when $0 \leq \theta \leq 1/2$.

Firstly, we give the proof of the following Lemma.

Lemma A.1 For $a_n^{(-\alpha)} = \frac{\Gamma(n+\alpha)}{\Gamma(\alpha)\Gamma(n+1)}$ and $0 < \alpha < 1$, we have

$$\left(\frac{1+\alpha}{2}\right)^j a_{n-j}^{(-\alpha)} \leq a_n^{(-\alpha)}, \quad 0 \leq j \leq n-1, \quad (\text{A.1})$$

$$a_n^{(-\alpha-1)} - a_n^{(-\alpha)} \leq (1+\alpha) \left(\frac{2+\alpha}{2}\right)^{n-2}, \quad n \geq 0. \quad (\text{A.2})$$

Proof. From $a_n^{(-\alpha)} = \frac{\Gamma(n+\alpha)}{\Gamma(\alpha)\Gamma(n+1)}$, we obtain $a_n^{(-\alpha-1)} - a_n^{(-\alpha)} = \frac{n}{\alpha} a_n^{(-\alpha)}$ and

$$\frac{a_{n+1}^{(-\alpha)}}{a_n^{(-\alpha)}} = \frac{n+\alpha}{n+1} \geq \frac{1+\alpha}{2}, \quad n \geq 1, \quad (\text{A.3})$$

$$\frac{a_{n+1}^{(-\alpha-1)} - a_{n+1}^{(-\alpha)}}{a_n^{(-\alpha-1)} - a_n^{(-\alpha)}} = \frac{n+\alpha}{n} \leq \frac{2+\alpha}{2}, \quad n \geq 2. \quad (\text{A.4})$$

Eq. (A.3) implies $\frac{a_n^{(-\alpha)}}{a_{n-j}^{(-\alpha)}} = \prod_{k=n-j}^{n-1} \frac{a_{k+1}^{(-\alpha)}}{a_k^{(-\alpha)}} \geq \left(\frac{1+\alpha}{2}\right)^j$, which completes the proof of (A.1). Obviously, (A.2) holds for $n = 0, 1$. From (A.4), we obtain $a_n^{(-\alpha-1)} - a_n^{(-\alpha)} \leq \left(\frac{2+\alpha}{2}\right)^{n-2} (a_2^{(-\alpha-1)} - a_2^{(-\alpha)}) = (\alpha+1) \left(\frac{2+\alpha}{2}\right)^{n-2}$. The proof complete. \square

For $0 \leq \theta \leq 1/2$, we have the following properties

$$f_1(\theta) = \frac{\theta}{1+\theta\alpha} + \frac{1-2\theta}{3-2\theta} \leq f_1((2+2\alpha)^{-1}) = \frac{1+\alpha}{2+3\alpha}, \quad (\text{A.5})$$

$$f_2(\theta) = 3\theta^2 \left(\frac{1-2\theta}{3-2\theta}\right) + \left(\frac{\theta}{1+\theta}\right)^3 + \left(\frac{1-2\theta}{3-2\theta}\right)^3 < \frac{8}{100}, \quad (\text{A.6})$$

$$f_3(\theta) = 4\theta \left(\frac{1-2\theta}{3-2\theta}\right)^2 + \left(\frac{\theta}{1+\theta}\right)^3 + \left(\frac{1-2\theta}{3-2\theta}\right)^3 < \frac{8}{100}, \quad (\text{A.7})$$

$$f_4(\theta) = \theta \frac{1-2\theta}{3-2\theta} + \frac{3}{8} \left[\frac{\theta^2}{(1+\theta)^2} + \left(\frac{1-2\theta}{3-2\theta}\right)^2 \right] < \frac{9}{100}, \quad (\text{A.8})$$

$$\rho_1 = \frac{1-2\theta}{3-2\theta} \leq \frac{1}{3}, \quad \rho_2 = \frac{\alpha\theta}{1+\alpha\theta} \leq \frac{\alpha}{2+\alpha}, \quad (\text{A.9})$$

where we used

$$\begin{aligned} \max_{0 \leq \theta \leq 1/2} f_1(\theta) &= f_1((2+2\alpha)^{-1}), & \max_{0 \leq \theta \leq 1/2} f_2(\theta) &\approx f_2(0.3769) \approx 0.0685, \\ \max_{0 \leq \theta \leq 1/2} f_3(\theta) &\approx f_3(0.1681) \approx 0.0602, & \max_{0 \leq \theta \leq 1/2} f_4(\theta) &\approx f_4(0.2811) \approx 0.0806. \end{aligned}$$

Proof. From (2.19) and (4.2), we have $c_n = 2b_0 a_n^{(-\alpha)} - \sum_{j=0}^n b_j a_{n-j}^{(-\alpha)}$, where b_n is given by (4.3).

Step 1) Prove $c_n \geq 0$ for $n \geq 3$. Let

$$\rho = \max\{\rho_1, \rho_2\}, \quad \rho_3 = \rho(2+\alpha)/2, \quad \lambda = (1+\alpha)/2. \quad (\text{A.10})$$

By (4.3), (A.10), (A.2), and $\sum_{j=1}^{n-1} a_j^{(-\alpha)} = a_n^{(-\alpha-1)} - 1 - a_n^{(-\alpha)}$, we have

$$\begin{aligned} b_n/b_0 &= \rho_1 \rho_2 \sum_{j=1}^{n-1} a_j^{(-\alpha)} \rho_1^{j-1} \rho_2^{n-j-1} + \rho_2^n + \rho_1^n a_n^{(-\alpha)} \\ &\leq \rho_1 \rho_2 \rho^{n-2} \sum_{j=1}^{n-1} a_j^{(-\alpha)} + \rho_2^n + \rho_1^n a_n^{(-\alpha)} \\ &\leq (1+\alpha) \rho_1 \rho_2 \rho_3^{n-2} + \rho_2^n + \rho_1^n a_n^{(-\alpha)}. \end{aligned} \quad (\text{A.11})$$

26 *H. Zhang et al.*

From (A.1), we have $\lambda^{1-n}a_n^{(-\alpha)}/\alpha \geq 1$ for $n \geq 1$. Hence,

$$\begin{aligned} b_n/b_0 &\leq [(1+\alpha)\rho_1\rho_2\rho_3^{n-2} + \rho_2^n] \lambda^{1-n}a_n^{(-\alpha)}/\alpha + \rho_1^n a_n^{(-\alpha)} \\ &= \left[\frac{1+\alpha}{\alpha\lambda} \rho_1\rho_2 \left(\frac{\rho_3}{\lambda}\right)^{n-2} + \frac{\lambda}{\alpha} \left(\frac{\rho_2}{\lambda}\right)^n + \rho_1^n \right] a_n^{(-\alpha)} \\ &\leq \left[\frac{1+\alpha}{\alpha\lambda} \rho_1\rho_2 \left(\frac{\rho_3}{\lambda}\right) + \frac{\lambda}{\alpha} \left(\frac{\rho_2}{\lambda}\right)^3 + \rho_1^3 \right] a_n^{(-\alpha)}, \quad n \geq 3, \end{aligned} \quad (\text{A.12})$$

where we used $\rho_1 \leq 1/3$, $\rho_2/\lambda < 1$, and $\rho_3/\lambda < 1$. Direct calculation yields

$$\frac{1+\alpha}{\alpha} \frac{\rho_1\rho_2\rho_3}{\lambda^2} = \begin{cases} \frac{2\alpha(2+\alpha)}{1+\alpha} \frac{1-2\theta}{3-2\theta} \frac{\theta^2}{(1+\alpha\theta)^2} \leq 3\theta^2 \frac{1-2\theta}{3-2\theta}, & \rho_1 \leq \rho_2, \\ \frac{2(2+\alpha)}{1+\alpha} \left(\frac{1-2\theta}{3-2\theta}\right)^2 \frac{\theta}{1+\alpha\theta} \leq 4\theta \left(\frac{1-2\theta}{3-2\theta}\right)^2, & \rho_1 > \rho_2, \end{cases} \quad (\text{A.13})$$

$$\frac{1}{\alpha} \frac{\rho_2^3}{\lambda^2} + \rho_1^3 = \frac{4\alpha^2}{(1+\alpha)^2} \frac{\theta^3}{(1+\theta\alpha)^3} + \left(\frac{1-2\theta}{3-2\theta}\right)^3 \leq \left(\frac{\theta}{1+\theta}\right)^3 + \left(\frac{1-2\theta}{3-2\theta}\right)^3. \quad (\text{A.14})$$

Combining (A.12), (A.13), (A.14), (A.6), and (A.7) yields

$$b_n/b_0 \leq \max\{f_2(\theta), f_3(\theta)\} a_n^{(-\alpha)} \leq \frac{2}{25} a_n^{(-\alpha)}, \quad n \geq 3. \quad (\text{A.15})$$

From (A.5), we have

$$b_1/b_0 = \rho_2 + a_1^{(-\alpha)} \rho_1 = \alpha \left(\frac{\theta}{1+\theta\alpha} + \frac{1-2\theta}{3-2\theta} \right) \leq \frac{\alpha(1+\alpha)}{2+3\alpha}. \quad (\text{A.16})$$

Combining (A.15) and (A.16) yields

$$\frac{b_0 a_n^{(-\alpha)} + b_1 a_{n-1}^{(-\alpha)} + b_n}{b_0 a_n^{(-\alpha)}} \leq \frac{27}{25} + \frac{3\alpha(1+\alpha)}{(2+\alpha)(2+3\alpha)} \leq \frac{27}{25} + \frac{2}{5} = \frac{37}{25}. \quad (\text{A.17})$$

where we used $a_{n-1}^{(-\alpha)} \leq \frac{n}{n-1+\alpha} a_n^{(-\alpha)} \leq \frac{3}{2+\alpha} a_n^{(-\alpha)}$ for $n \geq 3$.

Using (A.9), we obtain

$$\begin{aligned} 1 + \alpha - 2\rho_1 &\geq 1 + \alpha - 2/3 = (1 + 3\alpha)/3, \\ 1 + \alpha - 2\rho_2 &\geq 1 + \alpha - 2\alpha/(2 + \alpha) = (\alpha^2 + \alpha + 2)/(2 + \alpha), \\ 1 + \alpha - 2\rho_3 &\geq 1 + \alpha - \rho(2 + \alpha) \geq 1 + \alpha - (2 + \alpha)/3 = (1 + 2\alpha)/3, \end{aligned}$$

which leads to

$$\begin{aligned}
 & \frac{\rho_1\rho_2}{1+\alpha-2\rho_3} + \frac{1}{1+\alpha} \frac{\rho_2^2}{1+\alpha-2\rho_2} + \frac{\alpha}{2} \frac{\rho_1^2}{1+\alpha-2\rho_1} \\
 & \leq \frac{3\alpha}{1+2\alpha} \frac{\theta}{1+\theta\alpha} \frac{1-2\theta}{3-2\theta} + \frac{\alpha(2+\alpha)}{(1+\alpha)(2+\alpha+\alpha^2)} \frac{\alpha\theta^2}{(1+\alpha\theta)^2} \\
 & \quad + \frac{3\alpha}{2(1+3\alpha)} \left(\frac{1-2\theta}{3-2\theta} \right)^2 \\
 & \leq \theta \frac{1-2\theta}{3-2\theta} + \frac{3}{8} \left[\frac{\alpha\theta^2}{(1+\alpha\theta)^2} + \left(\frac{1-2\theta}{3-2\theta} \right)^2 \right] \\
 & \leq \theta \frac{1-2\theta}{3-2\theta} + \frac{3}{8} \left[\frac{\theta^2}{(1+\theta)^2} + \left(\frac{1-2\theta}{3-2\theta} \right)^2 \right] < \frac{9}{100}. \quad (\text{By (A.8)}) \quad (\text{A.18})
 \end{aligned}$$

From (A.11), $a_j^{(-\alpha)} \leq a_2^{(-\alpha)} = \alpha(1+\alpha)/2$, and the following inequality,

$$\begin{aligned}
 \sum_{j=2}^{n-1} \rho_k^j a_{n-j}^{(-\alpha)} &= \sum_{j=2}^{n-1} \frac{\rho_k^j}{\lambda^j} \left(\lambda^j a_{n-j}^{(-\alpha)} \right) \leq a_n^{(-\alpha)} \sum_{j=2}^{n-1} \frac{\rho_k^j}{\lambda^j} \leq a_n^{(-\alpha)} \frac{\rho_k^2/\lambda^2}{1-\rho_k/\lambda} \\
 &= \frac{\rho_k^2}{\lambda(\lambda-\rho_k)} a_n^{(-\alpha)} = \frac{4\rho_k^2}{(1+\alpha)(1+\alpha-2\rho_k)} a_n^{(-\alpha)}, \quad k=1,2,3,
 \end{aligned}$$

we obtain

$$\begin{aligned}
 \sum_{j=2}^{n-1} \frac{b_j}{b_0} a_{n-j}^{(-\alpha)} &\leq \sum_{j=2}^{n-1} \left[(1+\alpha)\rho_1\rho_2\rho_3^{j-2} + \rho_2^j + \frac{\alpha(1+\alpha)}{2}\rho_1^j \right] a_{n-j}^{(-\alpha)} \\
 &\leq 4 \left(\frac{\rho_1\rho_2}{1+\alpha-2\rho_3} + \frac{1}{1+\alpha} \frac{\rho_2^2}{1+\alpha-2\rho_2} + \frac{\alpha}{2} \frac{\rho_1^2}{1+\alpha-2\rho_1} \right) a_n^{(-\alpha)} \\
 &\leq \frac{9}{25} a_n^{(-\alpha)}. \quad (\text{By (A.18)}) \quad (\text{A.19})
 \end{aligned}$$

Combining (A.17) and (A.19) yields

$$b_0^{-1} \sum_{j=0}^n b_j a_{n-j}^{(-\alpha)} = \sum_{j=2}^{n-1} (b_j/b_0) a_{n-j}^{(-\alpha)} + (b_0 a_n^{(-\alpha)} + b_1 a_{n-1}^{(-\alpha)} + b_n) / b_0 \leq \frac{46}{25} a_n^{(-\alpha)},$$

which leads to

$$c_n = 2b_0 a_n^{(-\alpha)} - b_0^{-1} \sum_{j=0}^n b_j a_{n-j}^{(-\alpha)} \geq b_0 \left(2 - \frac{46}{25} \right) a_n^{(-\alpha)} = \frac{4}{25} b_0 a_n^{(-\alpha)} \geq 0, \quad n \geq 3.$$

Step 2) Prove $c_n > 0$ for $n = 0, 1, 2$. Obviously, $c_0 = 2b_0 - b_0 \geq b_0 > 0$ and

$$c_1 = (2-\alpha)b_0 - b_1 \geq \left(2 - \alpha - \frac{\alpha+\alpha^2}{2+3\alpha} \right) b_0 = \frac{4(1-\alpha^2)+3\alpha}{2+3\alpha} b_0 > 0,$$

where we used (A.16). By (A.5) and (A.9), we obtain

$$b_2/b_0 = \frac{\alpha^2\theta}{1+\theta\alpha} f_1(\theta) + \frac{\alpha(1+\alpha)}{2} \left(\frac{1-2\theta}{3-2\theta} \right)^2 \leq \frac{\alpha^2}{2+\alpha} \frac{1+\alpha}{2+3\alpha} + \frac{\alpha(1+\alpha)}{2} \frac{1}{9}.$$

28 *H. Zhang et al.*

From the above inequality and (A.16), we have

$$\begin{aligned}
 c_2/b_0 &= a_2^{(-\alpha)} - ((b_1/b_0)\alpha + b_2/b_0) \\
 &\geq \frac{\alpha(1+\alpha)}{2} - \left(\frac{\alpha^2(1+\alpha)}{2+3\alpha} + \frac{\alpha^2}{2+\alpha} \frac{1+\alpha}{2+3\alpha} + \frac{\alpha(1+\alpha)}{2} \frac{1}{9} \right) \\
 &= \alpha(1+\alpha) \left(\frac{4}{9} - \frac{\alpha}{2+3\alpha} - \frac{\alpha}{(2+\alpha)(2+3\alpha)} \right) \\
 &\geq \alpha(1+\alpha) \left(\frac{4}{9} - \frac{1}{5} - \frac{1}{15} \right) = \frac{8\alpha(1+\alpha)}{45} > 0.
 \end{aligned}$$

The proof is complete. \square

Appendix B. Proofs of Lemmas 3.2 and 3.6

Proof of Lemma 3.2.

Proof. For $\sigma \geq 0$, (3.4) follows from $\sum_{j=1}^{n-1} (n-j)^{-\alpha-1} j^\sigma \leq n^\sigma \sum_{j=1}^{n-1} (n-j)^{-\alpha-1} \lesssim n^\sigma \sum_{j=1}^{\infty} j^{-\alpha-1} \lesssim n^\sigma$. Next, we prove (3.4) for $\sigma < 0$.

For $n \geq 2$, there exists $j_n = \lceil n/2 \rceil$ and $x_0 = j_n/n \in (0, 1)$ such that

$$\begin{aligned}
 \sum_{j=1}^{n-1} (n-j)^{-\alpha-1} j^\sigma &= \sum_{j=1}^{j_n} (n-j)^{-\alpha-1} j^\sigma + \sum_{j=j_n+1}^{n-1} (n-j)^{-\alpha-1} j^\sigma \\
 &\leq \sum_{j=1}^{j_n} (n-j_n)^{-\alpha-1} j^\sigma + \sum_{j=j_n+1}^{n-1} (n-j)^{-\alpha-1} j_n^\sigma \\
 &\lesssim n^{-\alpha-1} \sum_{j=1}^{n-1} j^\sigma + n^\sigma \sum_{j=1}^{n-1} j^{-\alpha-1}.
 \end{aligned}$$

Using $\sum_{j=1}^{n-1} j^{-\alpha-1} \lesssim 1$ and $\sum_{j=1}^{n-1} j^\sigma \lesssim n^{\sigma+1} \log(n)$ completes the proof of (3.4).

By $0 \leq a_n^{(-\alpha)} \lesssim n^{\alpha-1}$, one has

$$\sum_{j=1}^n a_{n-j}^{(-\alpha)} j^\sigma \lesssim n^\sigma + \sum_{j=1}^{n-1} (n-j)^{\alpha-1} j^\sigma.$$

Repeating the proof of (3.4) finishes the proof of (3.5). The proof is completed. \square

Proof of Lemma 3.6.

Proof. The condition (2.5) and Lemma 2.1 yield the following linear system

$$\begin{aligned}
 \sum_{j=1}^m w_{n,j}^{(m)} j^{\sigma_k} &= \frac{\Gamma(\sigma_k + 1)}{\Gamma(\sigma_k + 1 - \alpha)} n^{\sigma_k - \alpha} - \sum_{j=1}^n \omega_{n-j}^{(\alpha)} j^{\sigma_k} \\
 &= O(n^{-\alpha-1}) + O(n^{\sigma_k - \alpha - p}), \quad 1 \leq k \leq m,
 \end{aligned}$$

which leads to

$$|w_{n,k}^{(m)}| \lesssim n^{-\alpha-1} + n^{\sigma_m-p-\alpha}, \quad 1 \leq k \leq m. \quad (\text{B.1})$$

Combining (3.8), Lemma 3.2, $\omega_n^{(\alpha)} = O(n^{-\alpha-1})$, (2.20), and (B.1) leads to

$$|W_{n,k}^{(m)}| \lesssim n^{\max\{-\alpha-1, \sigma_m-p-\alpha\}}, \quad 1 \leq k \leq m. \quad (\text{B.2})$$

Combining (3.2), (3.5), and (B.2) yields (3.15), which ends the proof. \square

Appendix C. Proof of Theorem 5.1

Proof. We show a sketch of the proof. Let $\theta^n = F u_h^n - u_h^n$. By (5.6), (2.15), and $\theta^n = \varepsilon_n = 0$ for $0 \leq n \leq n_0 - 1$, we obtain

$$\begin{aligned} \frac{1}{\tau^\alpha} \sum_{j=n_0}^n \omega_{n-j}^{(\alpha)}(\theta^j, v) + (\nabla \theta^n, \nabla v) &= (P_h(f(F u_h^n) - f(u_h^n)), v) \\ &\quad - \frac{1}{\tau^\alpha} \sum_{j=1}^{n-n_0} \varepsilon_{n-j} \omega_{n-j}^{(\alpha)}(\theta^j + u_h^j - u_h^0, v). \end{aligned} \quad (\text{C.1})$$

Similar to (3.19), we can obtain the equivalent form of (C.1) as

$$(\mathcal{A}_\tau^{\alpha, n_0-1} \theta^n, v) + (\mathcal{B}^{\alpha, n_0-1} \nabla \theta^j, \nabla v) = (\mathcal{B}^{\alpha, n_0-1} \tilde{F}^n, v) - \sum_{j=n_0}^n \tilde{b}_{n-j}(\theta^j, v) - (H^n, v). \quad (\text{C.2})$$

where $\tilde{F}^n = f(F u_h^n) - f(u_h^n)$, and

$$\tilde{b}_n = \frac{1}{\tau^\alpha} \sum_{j=n_0}^n b_{n-j} \varepsilon_j \omega_j^{(\alpha)}, \quad H^n = \sum_{k=n_0}^n b_{n-k} \sum_{j=1}^{k-n_0} \varepsilon_{k-j} \omega_{k-j}^{(\alpha)}(u_h^j - u_h^0).$$

By $\omega_n^{(\alpha)} = O(n^{-\alpha-1})$ and (3.4), we can easily obtain

$$|\tilde{b}_n| \lesssim \varepsilon n^{-\alpha-1}.$$

By the boundedness of $\|u_h^n\|$, $b_n = O(n^{-\alpha-1})$, and $\omega_n^{(\alpha)} = O(n^{-\alpha-1})$, we derive

$$\|H^n\| \lesssim \sum_{k=n_0}^n |b_{n-k}| \sum_{j=1}^k |\varepsilon_{k-j} \omega_{k-j}^{(\alpha)}| \lesssim \varepsilon \sum_{j=n_0}^n |b_{n-k}| \lesssim \varepsilon.$$

Following the proof of Theorem 2.2, we can easily arrive at (5.8), the details are omitted. The proof is complete. \square

Acknowledgment

The authors are grateful to Professor Dongfang Li for his valuable comments on an earlier version of this paper. This work has been supported by the National Natural Science Foundation of China (12001326, 11771254), Natural Science Foundation of Shandong Province (ZR2019ZD42, ZR2020QA032), China Postdoctoral Science Foundation (BX20190191, 2020M672038), the startup fund from Shandong University (11140082063130). GEK would like to acknowledge support by the MURI/ARO on Fractional PDEs for Conservation Laws and Beyond: Theory, Numerics and Applications (W911NF-15-1-0562)."

References

1. Multiprecision computing toolbox, *Advanpix, Tokyo* <http://www.advanpix.com>.
2. M. Al-Maskari and S. Karaa, Numerical approximation of semilinear subdiffusion equations with nonsmooth initial data, *SIAM J. Numer. Anal.* **57** (2019) 1524–1544.
3. A. A. Alikhanov, A new difference scheme for the time fractional diffusion equation, *J. Comput. Phys.* **280** (2015) 424–438.
4. D. Baffet and J. S. Hesthaven, A kernel compression scheme for fractional differential equations, *SIAM J. Numer. Anal.* **55** (2017) 496–520.
5. L. Banjai and M. López-Fernández, Efficient high order algorithms for fractional integrals and fractional differential equations, *Numer. Math.* **141** (2019) 289–317.
6. W. Bao and Y. Cai, Uniform error estimates of finite difference methods for the nonlinear Schrödinger equation with wave operator, *SIAM J. Numer. Anal.* **50** (2012) 492–521.
7. S. C. Brenner and L. R. Scott, *The mathematical theory of finite element methods*, volume 15 of *Texts in Applied Mathematics* (Springer, New York, 2008), third edition.
8. H. Brunner and T. Tang, Polynomial spline collocation methods for the nonlinear Basset equation, *Comput. Math. Appl.* **18** (1989) 449–457.
9. J. Cao and C. Xu, A high order schema for the numerical solution of the fractional ordinary differential equations, *J. Comput. Phys.* **238** (2013) 154–168.
10. L. Chen, J. Zhang, J. Zhao, W. Cao, H. Wang and J. Zhang, An accurate and efficient algorithm for the time-fractional molecular beam epitaxy model with slope selection, *Comput. Phys. Commun.* **245** (2019) 106842.
11. E. Cuesta, C. Lubich and C. Palencia, Convolution quadrature time discretization of fractional diffusion-wave equations, *Math. Comp.* **75** (2006) 673–696 (electronic).
12. K. Diethelm, J. M. Ford, N. J. Ford and M. Weilbeer, Pitfalls in fast numerical solvers for fractional differential equations, *J. Comput. Appl. Math.* **186** (2006) 482–503.
13. J. Dixon and S. McKee, Weakly singular discrete Gronwall inequalities, *Z. Angew. Math. Mech.* **66** (1986) 535–544.
14. Q. Du, J. Yang and Z. Zhou, Time-fractional Allen-Cahn equations: analysis and numerical methods, *J. Sci. Comput.* **85** (2020) Paper No. 42, 30.
15. C. González and C. Palencia, Stability of Runge-Kutta methods for abstract time-dependent parabolic problems: the Hölder case, *Math. Comp.* **68** (1999) 73–89.
16. L. Guo, F. Zeng, I. Turner, K. Burrage and G. E. Karniadakis, Efficient multistep methods for tempered fractional calculus: Algorithms and simulations, *SIAM J. Sci. Comput.* **41** (2019) A2510–A2535.
17. S. Jiang, J. Zhang, Q. Zhang and Z. Zhang, Fast evaluation of the Caputo fractional derivative and its applications to fractional diffusion equations, *Commun. Comput. Phys.* **21** (2017) 650–678.

18. B. Jin, B. Li and Z. Zhou, Correction of high-order BDF convolution quadrature for fractional evolution equations, *SIAM J. Sci. Comput.* **39** (2017) A3129–A3152.
19. B. Jin, B. Li and Z. Zhou, An analysis of the Crank-Nicolson method for subdiffusion, *IMA J. Numer. Anal.* **38** (2018) 518–541.
20. B. Jin, B. Li and Z. Zhou, Numerical analysis of nonlinear subdiffusion equations, *SIAM J. Numer. Anal.* **56** (2018) 1–23.
21. K. N. Le, W. McLean and K. Mustapha, Numerical solution of the time-fractional Fokker-Planck equation with general forcing, *SIAM J. Numer. Anal.* **54** (2016) 1763–1784.
22. B. Li and W. Sun, Unconditional convergence and optimal error estimates of a Galerkin-mixed FEM for incompressible miscible flow in porous media, *SIAM J. Numer. Anal.* **51** (2013) 1959–1977.
23. C. Li, Q. Yi and A. Chen, Finite difference methods with non-uniform meshes for nonlinear fractional differential equations, *J. Comput. Phys.* **316** (2016) 614–631.
24. D. Li, H.-l. Liao, W. Sun, J. Wang and J. Zhang, Analysis of L_1 -Galerkin FEMs for time-fractional nonlinear parabolic problems, *Commun. Comput. Phys.* **24** (2018) 86–103.
25. D. Li, J. Zhang and Z. Zhang, Unconditionally optimal error estimates of a linearized Galerkin method for nonlinear time fractional reaction-subdiffusion equations, *J. Sci. Comput.* **76** (2018) 848–866.
26. H. Li, X. Wu and J. Zhang, Numerical solution of the time-fractional sub-diffusion equation on an unbounded domain in two-dimensional space, *East Asian J. Appl. Math.* **7** (2017) 439–454.
27. J.-R. Li, A fast time stepping method for evaluating fractional integrals, *SIAM J. Sci. Comput.* **31** (2010) 4696–4714.
28. H.-l. Liao, D. Li and J. Zhang, Sharp error estimate of the nonuniform L_1 formula for linear reaction-subdiffusion equations, *SIAM J. Numer. Anal.* **56** (2018) 1112–1133.
29. H.-l. Liao, W. McLean and J. Zhang, A discrete Grönwall inequality with applications to numerical schemes for subdiffusion problems, *SIAM J. Numer. Anal.* **57** (2019) 218–237.
30. H.-l. Liao, Y. Yan and J. Zhang, Unconditional convergence of a fast two-level linearized algorithm for semilinear subdiffusion equations, *J. Sci. Comput.* **80** (2019) 1–25.
31. Y. Lin and C. Xu, Finite difference/spectral approximations for the time-fractional diffusion equation, *J. Comput. Phys.* **225** (2007) 1533–1552.
32. M. López-Fernández, C. Lubich and A. Schädle, Adaptive, fast, and oblivious convolution in evolution equations with memory, *SIAM J. Sci. Comput.* **30** (2008) 1015–1037.
33. C. Lubich, Discretized fractional calculus, *SIAM J. Math. Anal.* **17** (1986) 704–719.
34. Y. Luchko, Initial-boundary-value problems for the one-dimensional time-fractional diffusion equation, *Fract. Calc. Appl. Anal.* **15** (2012) 141–160.
35. I. Podlubny, *Fractional Differential Equations* (Academic Press, Inc., San Diego, CA, 1999).
36. J. Shen, T. Tang and L.-L. Wang, *Spectral methods*, volume 41 of *Springer Series in Computational Mathematics* (Springer, Heidelberg, 2011), algorithms, analysis and applications.
37. M. Stynes, E. O’Riordan and J. L. Gracia, Error analysis of a finite difference method on graded meshes for a time-fractional diffusion equation, *SIAM J. Numer. Anal.* **55** (2017) 1057–1079.
38. J. Sun, D. Nie and W. Deng, Fast algorithms for convolution quadrature of Riemann-Liouville fractional derivative, *Appl. Numer. Math.* **145** (2019) 384–410.

32 *H. Zhang et al.*

39. Z.-z. Sun and X. Wu, A fully discrete difference scheme for a diffusion-wave system, *Appl. Numer. Math.* **56** (2006) 193–209.
40. W. Tian, H. Zhou and W. Deng, A class of second order difference approximations for solving space fractional diffusion equations, *Math. Comp.* **84** (2015) 1703–1727.
41. L. Trefethen and J. Weideman, The exponentially convergent trapezoidal rule, *SIAM Review* **56** (2014) 385–458.
42. D. Wang and J. Zou, Dissipativity and contractivity analysis for fractional functional differential equations and their numerical approximations, *SIAM J. Numer. Anal.* **57** (2019) 1445–1470.
43. K. Wang and Z. Zhou, High-order time stepping schemes for semilinear subdiffusion equations, *SIAM J. Numer. Anal.* **58** (2020) 3226–3250.
44. Y. Yan, M. Khan and N. J. Ford, An analysis of the modified L1 scheme for time-fractional partial differential equations with nonsmooth data, *SIAM J. Numer. Anal.* **56** (2018) 210–227.
45. Y. Yang and F. Zeng, Numerical analysis of linear and nonlinear time-fractional subdiffusion equations, *Commun. Appl. Math. Comput.* **1** (2019) 621–637.
46. B. Yin, Y. Liu, H. Li and Z. Zhang, Finite element methods based on two families of second-order numerical formulas for the fractional cable model with smooth solutions, *J. Sci. Comput.* **84** (2020) Paper No. 2, 22.
47. F. Zeng, C. Li, F. Liu and I. Turner, Numerical algorithms for time-fractional subdiffusion equation with second-order accuracy, *SIAM J. Sci. Comput.* **37** (2015) A55–A78.
48. F. Zeng, I. Turner, K. Burrage and G. E. Karniadakis, A new class of semi-implicit methods with linear complexity for nonlinear fractional differential equations, *SIAM J. Sci. Comput.* **40** (2018) A2986–A3011.
49. F. Zeng, Z. Zhang and G. E. Karniadakis, Second-order numerical methods for multi-term fractional differential equations: Smooth and non-smooth solutions, *Comput. Methods Appl. Mech. Engrg.* **327** (2017) 478–502.
50. H. Zhu and C. Xu, A fast high order method for the time-fractional diffusion equation, *SIAM J. Numer. Anal.* **57** (2019) 2829–2849.

This figure "alf02t1.jpg" is available in "jpg" format from:

<http://arxiv.org/ps/2007.07015v2>

This figure "alf05t1.jpg" is available in "jpg" format from:

<http://arxiv.org/ps/2007.07015v2>

This figure "alf08t1.jpg" is available in "jpg" format from:

<http://arxiv.org/ps/2007.07015v2>

This figure "fig1-h01.jpg" is available in "jpg" format from:

<http://arxiv.org/ps/2007.07015v2>

This figure "fig2-h01.jpg" is available in "jpg" format from:

<http://arxiv.org/ps/2007.07015v2>

This figure "alf02t5.jpg" is available in "jpg" format from:

<http://arxiv.org/ps/2007.07015v2>

This figure "alf05t5.jpg" is available in "jpg" format from:

<http://arxiv.org/ps/2007.07015v2>

This figure "alf08t5.jpg" is available in "jpg" format from:

<http://arxiv.org/ps/2007.07015v2>

This figure "alf02t10.jpg" is available in "jpg" format from:

<http://arxiv.org/ps/2007.07015v2>

This figure "alf05t10.jpg" is available in "jpg" format from:

<http://arxiv.org/ps/2007.07015v2>

This figure "alf08t10.jpg" is available in "jpg" format from:

<http://arxiv.org/ps/2007.07015v2>

This figure "alf02t20.jpg" is available in "jpg" format from:

<http://arxiv.org/ps/2007.07015v2>

This figure "alf05t20.jpg" is available in "jpg" format from:

<http://arxiv.org/ps/2007.07015v2>

This figure "alf08t20.jpg" is available in "jpg" format from:

<http://arxiv.org/ps/2007.07015v2>